Smart electric vehicle charging for reducing photovoltaic energy curtailment

Electric Power Systems Research 230 (2024) 110181

Contents lists available at ScienceDirect

Electric Power Systems Research

journal homepage: www.elsevier.com/locate/epsr

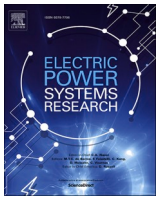

Smart electric vehicle charging for reducing photovoltaic energy curtailment

Soheil Saadatmandi [a], Gianfranco Chicco [a,*], Alfredo Favenza [b], Alessandro Mozzato [b], Francesco Giordano [b], Maurizio Arnone [b]

[a] Dipartimento Energia "Galileo Ferraris", Politecnico di Torino, Corso Duca degli Abruzzi 24, Torino 10129, Italy
[b] Links Foundation, via Pier Carlo Boggio 61, Torino 10138, Italy

ARTICLE INFO

Keywords:
Renewable energy
Photovoltaic systems
Curtailment
Electric vehicles
Smart charging
Blockchain

ABSTRACT

The increased diffusion of Photovoltaic (PV) generation could be limited by the grid capacity to host the power input from PV systems, especially in mid-day hours on sunny days. This paper proposes a framework of analysis to determine the mitigation of the PV energy curtailment in the grid, based on a novel smart charging strategy for electric vehicles (EVs) that operate in the grid-to-vehicle mode. This framework adopts a combination of methods and techniques, with a clustering procedure to group the EV charging stations with some PV systems based on the electrical distance, a novel smart charging strategy for the EVs based on the definition of fuzzy weights, and the exploitation of the blockchain technology with a Proof-of-Authority consensus protocol to reinforce network security and achieve decentralization. The blockchain provides full traceability of EV charging operations and grid status monitoring during time. The proposed framework contains novel indicators of avoided PV power reduction and energy curtailment. To account for the EV-related uncertainty, these indicators are determined from a Monte Carlo-based assessment of the three-phase power flow results. The results are presented on a three-phase unbalanced 123-node system with given locations of PV systems and EV charging stations.

1. Introduction

The exploitation of renewable energy sources (RES) is a viable option to reduce the harmful impact of the greenhouse gas emissions resulting from the use of fossil fuels as the primary source of energy generation. Photovoltaic (PV) installations are the dominant type of RES connected to the Medium Voltage (MV) or Low Voltage (LV) grids. The reduction in the production cost and the increase in the PV module efficiency that occurred in the last years enable progressive PV diffusion. On the global scale, the diffusion of PV installations is still limited, compared with the overall electricity needs. However, on a local scale, the power produced by PV installations could already exceed the local demand in some periods of time, especially in mid-day periods with a clear sky. In this case, the Distribution System Operator (DSO) needs to curtail some parts of the production from PV power plants to comply with the grid constraints, in order to avoid overcurrents in the network branches (lines and transformers) and/or over-voltages in some grid nodes [1]. A lack of suitable means to prevent PV generation curtailment leads to the wasting of energy produced by RES and raises issues about fairness of active power curtailment [2]. The extent of PV curtailment is not negligible [3], with percentages higher than 5% of the PV energy production occurred for example in Texas (8.4% in 2018 [3]) and in California (10% in the first four months of 2020 [4] and 6.3% in 2022 [5]). The report of the International Energy Agency [6] indicates that the curtailment of the energy produced from variable renewable energy (VRE) resources remains relatively low (from 1.5% to 4%) in most large renewable energy markets. However, the energy curtailment for VRE systems will likely increase with the expected growth in the VRE diffusion if the countries will not manage the renewable energy integration with appropriate measures, particularly with the expansion of the transmission and distribution networks and increasingly higher adoption of storage systems.

From the literature, the solutions proposed to tackle PV generation curtailment during operation typically fall into three major categories:

1) Development of control strategies to enhance the operation of PV systems by exploiting the active and reactive power control capabilities of the equipment available in the distribution network (e.g.,

* Corresponding author.
E-mail address: gianfranco.chicco@polito.it (G. Chicco).

https://doi.org/10.1016/j.epsr.2024.110181
Received 28 July 2023; Received in revised form 6 December 2023; Accepted 21 January 2024
Available online 15 February 2024

local control on the PV inverters, and control of capacitor banks and on-load tap changers of the transformers).

2) Designing battery energy storage systems (BESS) suitable for managing the energy produced by RES, by storing the excess of production into the batteries and supply the demand through the batteries in case of low or fluctuating production from RES. The presence of a local BESS could enable the local energy system to exploit the whole PV production by storing it into the BESS rather being curtailed. However, the costs of BESS systems are still relatively high, and their installation is not sufficiently scattered in the distribution systems to ensure that there will be no PV production curtailment.
3) Adapting the intermittent demand to receive the excess of PV generation, e.g. by rescheduling the on/off periods of appliances in residential areas based on different strategies during peak power generation hours or defining smart charging strategies for the electric vehicles (EVs) connected to the grid. Therefore, the excess energy injected by PV energy to the grid would be consumed and avoided to be curtailed, while satisfying the EV owner or user needs.

The main aspects referring to relevant solutions developed for these categories are based on the selected references critically reviewed below.

With reference to the first category indicated previously (control strategies), priority is given to the reduction of the related barriers through decentralized control of active and reactive power, leaving PV curtailment only as the last resort [7]. By analyzing the effectiveness of different control schemes, including centralized and decentralized control [8], the conclusion is that the most effective scheme is the volt-var operation mode, based on limiting the voltage increase at the point of grid connection of the PV system by controlling the reactive power based on local voltage measurement.

For the second category (BESS design), power shortfalls and PV curtailments in a power system with PV and BESS can be reduced by using a scheduling method [9]. From the results obtained through numerical simulations on the Kanto area of Japan, this methodology eliminates power shortfalls by 100% with the consideration of BESS in the grid and reduces PV energy curtailment to 69.5% and 95.2% in months of high and low solar irradiance, respectively. The calculation of the optimal size of a residential storage system takes into account the possible overvoltages that lead to PV energy curtailment in residential rooftops [10]. The method used considers energy curtailment, voltage levels, and the financial losses incurred by PV owners, because whenever PV energy curtailment occurs the owner incurs a financial loss due to lack of energy production. The method has been implemented for an 11 kV feeder in South Australia and the results suggest that PV energy curtailment could be reduced by 54.7% in case of installation of 100% optimally sized storage system on the grid. The charging and discharging of BESS scheduled in [11] reduces the PV curtailment based on the day-ahead and intraday few-hours-ahead forecast PV power outputs. Rescheduling the charge/discharge of the BESS based on more accurate intraday forecasts enables more efficient use of PV generation. Another solution is to set up a decentralized management method for a PV system equipped with the energy storage and a Power Conditioning System (PCS), considering real time pricing and distributed decision making [12]. In this case, a pricing signal is sent to each PCS at each time step and every PCS adjust their optimal set point for the output power as a solution to an individual optimization problem. This methodology has been assessed through numerical and real physical experiments carried out in Japan on a downscaled model with 1 kW capacity that represents the operation of the PCS on a PV system with 2.5 MW capacity, indicating that this method could also be used effectively in cases without batteries installed. Shared ESS charging and discharging, together with PV production curtailment, is addressed in [13], where the PV producers share the costs of the ESS infrastructure and distribute the profits based on power sensitivity allocation ratios.

The third category (demand adaptation) is the one of specific interest in this paper. The trend is to reduce PV energy curtailments by increasing the consumption inside the grid. The International Energy Agency [14] identifies the opportunity of EV participation for increasing local flexibility to support more variable renewable generation. Smart EV charging strategies could contribute to reduce RES curtailment up to 40% with respect to unmanaged EV charging [15]. In a LV distribution network with deep PV penetration, a voltage regulation strategy has been developed through a consensus-based cooperative of plug-in EVs (PEV) and PV active power curtailment [16]. Coordinated charging and discharging control of PEV batteries provides maximum utilization of the energy generated by PVs which is going to be curtailed to meet the grid constraints. The strategy has been verified to be feasible and versatile when EVs arrive or depart occasionally only, so that this strategy may not hold for frequent EV departures and arrivals. This approach assumes that each customer has both rooftop PV and PEV systems, while in practical cases this could not happen. EV charging with battery swapping is addressed in [17] for providing peak shaving in networks with variable production from PV and wind systems, where the uncertainty in the EV charging strategy is reduced by starting with a swapped EV battery. In the coordinated EV charging strategy presented in [4], a fitted Q-iteration algorithm has been considered, because it needs fewer learning steps. This algorithm is implemented on EVs to adjust the EV charging schedule by reinforcement relearning. This research is conducted in California based on three case studies that consider 100 EVs with similar battery ratings (5 kW maximum power) and capacity (16.67 kWh), and in all of them a fleet of EVs belong to an aggregator that exploits the charging strategy to achieve a certain goal. The studies are conducted without considering the distribution grid with its topology, generation, demand and constraints, which is a limiting factor, as other stakeholders may not be fully considered [18]. A model predictive control-based method that uses PV inverters reactive power compensation and EV active power charging is presented in [19] to provide flexibility in radial distribution systems, with testing conducted on the IEEE 123-bus system by considering a high penetration level with 30 PV systems and 25 EV aggregators. Sensitivity-based active power curtailment is addressed in [20] to mitigate voltage violations in a 45-bus European distribution network with 6 PV systems and 3 EV charging stations.

Various approaches found in the literature refer to centralized strategies applicable in the distribution grid. Coordinated actions carried out by multiple PV and EV aggregators are considered in [21] to provide an even partitioning of the PV power to be curtailed by all aggregators at each time step of analysis. In another EV coordinated charging method to consume PV energy production and avoid overvoltages in the low voltage distribution networks [22], every house is equipped with solar panels and each household owns an EV. In this case, in order to reduce PV energy curtailments by means of utilization of EVs, three main issues are considered: (i) determination of appropriate amount of EV charging shift, where inappropriate charging shift may cause extra costs for the users, since the excess amount energy produced by PVs could be sold to the grid; (ii) assurance of customer autonomy on charging their vehicles, and (iii) assurance of equity. The users who schedule their EV charging accordingly should receive greater benefits than those who do not. The bidders submit their bids in an algorithm-based manner according to the truthful bids for the target value. In the auction mechanism, the users voluntarily determine the bids without knowing the other's bids and compete to obtain the rights to carry out the EV charging shift. The winners of an auction shift their charging schedule and obtain the incentive as the summation of fees by other bidders in the network. The robustness of the methodology illustrated is evaluated through simulations carried out in both residential and industrial areas. The auction mechanism leads to a voluntary voltage reduction by shifting the charging period of EVs as well as PV output curtailment. Also in this case, situations in which EVs are not present in all locations with PV production, and hence with the consequence that the bidders cannot be uniformly present, are not considered. Moreover, in a valley-filling

approach with the contribution of EVs for the reduction of renewable energy curtailment [23], the simulation results on the Kyusyu area in Japan show that applying this approach could almost eliminate all renewable energy curtailments with 20% penetration of EVs. Different scenarios regarding the uncertainties such as EVs plug-in time and available charging/discharging capacity are also modelled. A further contribution from Japan considers the impact of different rated of EV diffusion and PV capacity for a planning period of 10 years. The authors conclude that with a sufficiently high EV diffusion (the scenarios analyzed consider from 300,000 to 570,000 EVs) it is possible to maintain the level of PV energy curtailed between 10% and 15% [24], however, additional improvements due to EV smart charging are not considered. The PV and EV hosting capacity is analyzed in [25] on the IEEE European Low Voltage test network, showing that PV curtailment does not improve the hosting capacity for EV, as well as that EV smart charging improves only slightly the PV hosting capacity. However, the benefits of EV smart charging for the operation of existing PV systems are not discussed in that study. A distributionally robust optimization is proposed in [26] for a distribution network operation under uncertainty conditions, where the network topology is considered, the demand curtailed is included in the objective function; however, the generation curtailment is not represented.

The scheduling of the respective EV charging can be seen as a service in the context of demand response strategies aimed at reducing PV energy curtailment and the corresponding economic losses. The transmission system operator sets out the requests and incentives, and the managing entity of the EV charging station decides how the EVs belonging to the charging station participate in the demand response action [27]. However, no type of uncertainty is taken into account. Other papers consider energy curtailment costs inside an objective function used for distribution system optimization. For example, a multi-objective coordinated charging model of EVs has been formulated in [28] by considering the maximum profit of the virtual power plant and the minimum variance of the distribution network load. Furthermore, an optimization problem has been set up in [29] by introducing a renewable power curtailment penalty cost and the waiting time cost for EV battery swapping. Addressing economic optimization aspects is outside the scope of this paper.

The emerging blockchain and distributed ledger technology (DLT) have attracted considerable interest in the energy sector, especially in smart grids, where integrating and coordinating a large number of growing connections can be a challenging issue for the traditional centralized grid systems [30]. Examples of application of blockchains in smart grids include solutions to control and manage increasingly decentralized complex energy systems [31] and charging stations [32], decentralized coordination and control for integration of distributed energy resources [33] and energy dispatching [34], innovative trading platforms where prosumers and consumers can trade their energy surplus on a peer-to-peer network [35] leveraging secure smart contracts [36], solutions to improve the resilience and the security of smart grids [37], decentralized systems to manage EV charging [38] and vehicle-to-grid power trading mechanisms in smart grids [39], and EV incentive system to maximize the utilization of renewable energy [40].

The integration of blockchain in the context of EV charging infrastructures is evolving. Conventional consensus algorithms have been included to manage transactions and guarantee decentralization and traceability of the payments [41]. Transactions are made based on bids that depend on forecasting different parameters [42]. Leveraging the distributed ledger technology for the EVs billing system is aimed at preventing malicious tampering on the transactions [43].

The smart charging methodologies introduced in [44,45] for the integration of PV energy and grid stabilization by means of energy storage systems (ESS) and EVs are based on scheduling EV charging to avoid overloads and peak load shaving. Smart EV charging infrastructures are proposed, as are ways to evaluate grid parameters such as charging demands and loads to provide best charging schedule and achieve energy price cutting and load congestion prevention. The references on the adaptation of blockchain for EV charging mainly exploit conventional consensus algorithms based on Proof of Stake (PoS). The algorithms that consider the charging power and grid parameters rely on the forecasts made based on the given parameters and ask the EV owners to charge in specific timing periods established by the algorithm to gain profits. In the original PoS, validators are selected based on the amount of stake (wealth) that they put and those with higher stakes tends to have a higher chance of being chosen to forge their blocks. Thus, wealthier members become wealthier in each round. This strategy might end up in a “nothing at the stake” congestion, which is a common drawback of a PoS algorithm [46]. Moreover, PoS consensus is typically adopted in public-permissionless blockchain solution, which could be inconvenient in smart grid applications where there could be the need for a more restricted and private control over users and transactions. In the proposed system, blockchain is running based on the proof of authority (PoA) algorithm. According to the literature [47], this consensus protocol is decentralized and improves the security of the system against malicious cyber-attacks. In addition, implementing this protocol, traceability and scalability are gained at the same time. It is also a private blockchain algorithm suitable for the proposed methodology.

From the indications provided above, setting up an overall framework of EV interaction with the grid for reducing the PV power curtailment is one of the current challenges. To fill the research gaps identified from the literature review, the main contribution provided in this paper is the formulation of an overall *framework* that features the following novelties:

- The PV generation curtailment is characterized in a three-phase unbalanced distribution grid, taking into account the grid constraints, with the definition of a reference case and of specific PV energy curtailment indicators.
- The effects of uncertainty on PV generation and with regard to EVs (type of EV, arrival time, departure time and initial state of charge) are addressed with a Monte Carlo-based approach by defining the new indicators *avoided PV energy curtailment effectiveness* and *PV peak power reduction effectiveness*.
- The smart charging of EVs is considered for grid-to-vehicle applications, proposing an EV smart charging strategy in which the EVs are supplied by the excess of PV production by increasing their charging power, scheduled for successive time steps. The proposed framework adopts a combination of methods and techniques (clustering, fuzzy logic and blockchain) and has a broader prospect with respect to the application of specific methodologies to solve individual aspects of PV generation curtailment as found in the current literature.
- The blockchain-based EV charging strategy proposed in this paper aims to address the reduction of PV energy curtailment during the peak power generation by exploiting EVs modelled as a dynamic battery. Therefore, the installation of expensive BESS in the grid can be avoided. In addition, EVs charge their batteries with higher charging power when needed to reduce PV curtailment, thus reducing their charging time. The proposed strategy works properly regardless of the type of EV charger used in the charging infrastructures and time of the day. It also does not involve EV owners in the charging process. EV owners benefit from the excess energy generated by PVs without paying extra costs.

To confirm the effectiveness of the proposed approach, simulations are carried out on a three-phase unbalanced distribution system with different numbers of charging points inside the network.

The next sections of this paper are organized as follows. Section 2 presents the overall framework considered for addressing the cases with PV power curtailment. Section 3 illustrates the model used for EV smart charging. Section 4 is dedicated to the application to a distribution

network. The last section contains the concluding remarks.

2. Framework for assessing PV power curtailment

2.1. Main concepts

The possibility of avoiding PV power curtailment is analyzed by defining a reference case, in which all the available PV generation can be used in the system. This reference case is defined in the ideal situation in which no grid constraints are enforced. PV power curtailment is then assessed by imposing the grid constraints and calculating other solutions in which no violation of these constraints occurs under specific scenarios of climatic conditions and energy management inside the system. Different cases are addressed, by considering the type of day with reference to the climatic conditions (e.g., sunny or cloudy day), and the management strategies adopted. The analysis is carried out by taking daily demand and PV generation patterns with a specified time step of analysis. Changing the time step would lead to different results, because of the averaging effect that produces smoother power patterns when the time step duration increases [48].

In the *reference case*, the following quantities are observed, for a given day:

- The PV power $P_{\mathrm{PV}}^{\mathrm{ref}}(t)$ generated during time.
- The PV peak power $\widehat{P}_{\mathrm{PV}}^{\mathrm{ref}}$ reached during the day.
- The energy $W_{\mathrm{PV}}^{\mathrm{ref}}$ generated by the PV system in the day.

The other cases analyzed are denoted with the superscript $k = 1, \ldots, K$. The following quantities are of interest:

- The PV power $P_{\mathrm{PV}}^{(k)}(t)$ generated during time.
- The peak PV power $\widehat{P}_{\mathrm{PV}}^{(k)}$ reached during the day without violations of the grid limits.
- The PV energy $W_{\mathrm{PV}}^{(k)}$ generated by the PV system in the day without violations of the grid limits.
- The power reductions due to PV power curtailment during the day, obtained by taking only the positive values of the difference between the reference PV power and the PV power generated during time:

$$\Delta P_{\mathrm{PV}}^{(k)}(t) = \max\left\{P_{\mathrm{PV}}^{\mathrm{ref}}(t) - P_{\mathrm{PV}}^{(k)}(t),\ 0\right\} \tag{1}$$

- The cumulative distribution function $F(\Delta P_{\mathrm{PV}}^{(k)})$ of the PV power reductions due to PV power curtailment during the day, calculated by considering the exceeding probability of the values $\Delta P_{\mathrm{PV}}^{(k)}$ for all the cases with positive $\Delta P_{\mathrm{PV}}^{(k)}$.

2.2. PV energy curtailment indicators

The need for respecting grid limits causes the curtailment of the excess PV generation. The following indicators of PV curtailment are determined for case $k = 1, \ldots, K$:

1) The PV energy $W_{\mathrm{PV,cur}}^{(k)}$ curtailed during the day [49]:

$$W_{\mathrm{PV,cur}}^{(k)} = W_{\mathrm{PV}}^{\mathrm{ref}} - W_{\mathrm{PV}}^{(k)} \tag{2}$$

2) The peak power reduction $\widehat{P}_{\mathrm{PV,cur}}^{(k)}$ after PV curtailment, calculated by considering the peaks of PV generation in the reference case and in the case analyzed, which generally occur at different time steps:

$$\widehat{P}_{\mathrm{PV,cur}}^{(k)} = \widehat{P}_{\mathrm{PV}}^{\mathrm{ref}} - \widehat{P}_{\mathrm{PV}}^{(k)} \tag{3}$$

3) The maximum of the PV power reductions due to PV power curtailment during the day:

$$\widehat{P}_{\mathrm{PV,red}}^{(k)} = \max_{t}\left\{\Delta P_{\mathrm{PV}}^{(k)}(t)\right\} \tag{4}$$

4) The PV power reduction $P_{\mathrm{PV,red},\ x\%}^{(k)}$ due to PV power curtailment with exceeding probability $x\%$ during the day, which gives a less extreme indication than $\widehat{P}_{\mathrm{PV,red}}^{(k)}$ about the PV power reductions that occur during the period of analysis. The term $P_{\mathrm{PV,red},\ x\%}^{(k)}$ is determined as the value of $\Delta P_{\mathrm{PV}}^{(k)}$ such that $F(\Delta P_{\mathrm{PV}}^{(k)}) = x/100$. For example, $P_{\mathrm{PV,red},\ 5\%}^{(k)}$ is the PV power reduction that is exceeded for 5% of the cases in which there is a PV power curtailment.

The analysis is carried out on distribution systems, which typically operate in unbalanced conditions. The results are then analyzed based on the three-phase power flow calculations, to check the constraint satisfaction on each phase. The PV energy curtailment is taken as the sum of the PV energy curtailments that occurs over the three phases at each node of the grid where PV systems are in operation.

2.3. Uncertainty effects

Both PV generation and EV arrival are subject to uncertainty. However, the cases with higher PV energy curtailment occur on sunny days, in which the uncertainty in the PV production is low. Nevertheless, the uncertainty on the EV arrival and state of charge is generally higher. This aspect has been taken into account by executing, for the same weather conditions for PV generation, M simulations in the Monte Carlo framework, with different instances of the random variables associated to the EV arrival, initial state of charge and duration of the permanence at the charging point. The random variables are picked up from a uniform probability distribution in the specific ranges of variation established for each random variable. The time of the day for EV arrival is considered minute-by-minute. For the minimum and maximum initial state of charge of the EV battery, and minimum and maximum duration of permanence at the charging point, the limits of the ranges are specified in Section 4.1 for the case study.

Let us consider as random variable $\mathbf{r}$ of interest the indicators $W_{\mathrm{PV,cur}}^{(k)}$, $\widehat{P}_{\mathrm{PV,cur}}^{(k)}$, $\widehat{P}_{\mathrm{PV,red}}^{(k)}$ or $\widehat{P}_{\mathrm{PV,red},x\%}^{(k)}$, generated to correspond to independent random samples. The uncertainty on the estimation of the random variable is represented by the variance of the expected value, estimated by using the sample mean $\mathbb{E}_M\{\mathbf{r}\}$ and the sample variance $\sigma_M^2(\mathbf{r})$ determined after M Monte Carlo simulations:

$$\sigma_M^2(\mathbb{E}_M\{\mathbf{r}\}) = \frac{\sigma_M^2(\mathbf{r})}{M} \tag{5}$$

with the corresponding standard deviation:

$$\sigma_M(\mathbb{E}_M\{\mathbf{r}\}) = \frac{\sigma_M(\mathbf{r})}{\sqrt{M}} \tag{6}$$

Starting from an initial number of simulations $M-1$ (for M higher than a minimum value), with the calculation of the corresponding sample mean and sample variance according to the general definition, the update of the sample mean $\mathbb{E}_M\{\mathbf{r}\}$ and sample variance $\sigma_M^2(\mathbf{r})$ for

successive values of M can be carried out by considering the incremental expressions that avoid the full recalculation of the values from the general definition when M increases:

$$\mathbb{E}_M\{\mathbf{r}\} = \mathbb{E}_{M-1}\{\mathbf{r}\} + \frac{\mathbf{r}_M - \mathbb{E}_{M-1}\{\mathbf{r}\}}{M} \tag{7}$$

$$\sigma_M^2(\mathbf{r}) = \left(1 - \frac{1}{M-1}\right)\sigma_{M-1}^2(\mathbf{r}) + M(\mathbb{E}_M\{\mathbf{r}\} - \mathbb{E}_{M-1}\{\mathbf{r}\})^2 \tag{8}$$

From these values, a criterion for determining the termination of the Monte Carlo simulation, also used in power system problems where the outcomes depend on the extraction of many random variables [50], is based on the calculation of the coefficient of variation [51] after M simulations:

$$\beta_M = \frac{\sigma_M(\mathbb{E}_M\{\mathbf{r}\})}{\mathbb{E}_M\{\mathbf{r}\}} = \frac{\sigma_M(\mathbf{r})}{\mathbb{E}_M\{\mathbf{r}\}\sqrt{M}} \tag{9}$$

stopping the Monte Carlo simulation when the following condition is verified:

$$\beta_M < \varepsilon \tag{10}$$

where ε is the threshold considered in the stop criterion.

More in detail, confidence intervals can be considered. For a normal probability distribution of the outcomes, with $(1-\alpha)$*100% confidence, the confidence bounds are $\mathbb{E}\{\mathbf{r}\} \pm z_{\alpha/2}\,\sigma(\mathbf{r})/\sqrt{M}$ (e.g., the 95% confidence bounds correspond to $\alpha = 0.05$ and $z_{\alpha/2} = 1.96$, and the 99% confidence bounds correspond to $\alpha = 0.01$ and $z_{\alpha/2} = 2.58$). The stop criterion that determines the end of the Monte Carlo process after M simulations can be established when the following condition is verified [52]:

$$\frac{z_{\alpha/2}\sigma_M(\mathbf{r})}{\mathbb{E}_M\{\mathbf{r}\}\sqrt{M}} < \varepsilon_{\mathrm{MC}} \tag{11}$$

where the left-hand side of (11) is the Monte Carlo test error, and $\varepsilon_{\mathrm{MC}}$ is the threshold considered for convergence. The number of iterations M_{MC} is then the smallest number M that satisfies the condition (11).

If the Monte Carlo samples come from a non-normal distribution, the situation is more challenging [53] and many criteria have been proposed. In a simple case, the term $z_{\alpha/2}$ in (11) could be multiplied by an arbitrary (i.e., not supported by a rigorous approach) inflaction factor [54] higher than unity to represent a more conservative approximate confidence interval. In this paper, the Monte Carlo test error is tracked for different values of M for the random variables referring to curtailed energy and power. The variation of the Monte Carlo test error is also tracked to identify possible significant changes. On these bases, considering the numbers of iterations M_{MC} found in the different cases, a suitable number M^* of Monte Carlo simulations can be selected to carry out the further analyses indicated below.

The statistics of the results are shown as Cumulative Distribution Functions (CDFs) of the PV energy curtailed $W_{\mathrm{PV,cur}}^{(k)}$ defined in (2) and of $P_{\mathrm{PV,red},\,x\%}^{(k)}$ after PV curtailment defined in (4). Starting from these CDFs, specific indicators can be formulated to assess the effectiveness of the proposed strategy. A novel general framework is introduced here to construct these indicators. At first, the reference case of PV production is taken, with PV energy production $W_{\mathrm{PV}}^{\mathrm{ref}}$ and PV peak power $\widehat{P}_{\mathrm{PV}}^{\mathrm{ref}}$. Then, the $m = 1, \ldots, M^*$ occurrences of PV energy production $W_{\mathrm{PV},m}^{(k)}$ and PV power $P_{\mathrm{PV},m}^{(k)}(t)$ are determined from the M^* Monte Carlo simulations. Then, the $W_{\mathrm{PV,cur},m}^{(k)}$ and $\widehat{P}_{\mathrm{PV,red},m}^{(k)}$ are calculated from (2) and (4), respectively, and the corresponding Complementary Cumulative Distribution Functions (CCDFs) are formed.

In the ideal case, the PV energy production would be unchanged in all M^* occurrences with respect to $W_{\mathrm{PV}}^{\mathrm{ref}}$, and the PV peak power would then be always equal to $\widehat{P}_{\mathrm{PV}}^{\mathrm{ref}}$. Otherwise, there will be reductions in the PV energy production and in the PV peak power. The framework introduced compares the outcomes of the Monte Carlo simulations with the ideal case (in which the CCDF has all values equal to zero). Then, the difference between the CCDF obtained from Monte Carlo simulations and the ideal CCDF is represented by the area (qualitatively shown in Fig. 1 for a generic variable y) calculated as

$$A_y = \frac{1}{M^*}\sum_{m=1}^{M^*} y_m \tag{12}$$

On these bases, a new indicator of effectiveness of the solutions is introduced here as:

$$\xi_y = \frac{1}{1 + A_y} \tag{13}$$

The indicator ξ_y has its maximum value equal to 1 when all the occurrences of the Monte Carlo analysis are equal to the ideal case. Otherwise, the indicator ξ_y can be used to set up a relative comparison among the effects of applying different strategies to decrease PV curtailment. In particular, when $y = W_{\mathrm{PV,cur}}^{(k)}/W_{\mathrm{PV}}^{\mathrm{ref}}$, the area determined is A_W from (12) and the indicator is denoted as *Avoided PV energy curtailment effectiveness*:

$$\xi_W = \frac{1}{1 + A_W} \tag{14}$$

Moreover, when $y = \widehat{P}_{\mathrm{PV,red}}^{(k)}$ (to be expressed in per units), the area determined is $A_{\Delta\hat{P}}$ from (12) and the indicator is denoted as *PV peak power reduction effectiveness*:

$$\xi_{\Delta\hat{P}} = \frac{1}{1 + A_{\Delta\hat{P}}} \tag{15}$$

Finally, when $y = P_{\mathrm{PV,red},\,x\%}^{(k)}$ (to be expressed in per units), the area determined is $A_{\Delta P,x\%}$ from (12) and the indicator is denoted as *PV power reduction effectiveness at x%*:

$$\xi_{\Delta P,x\%} = \frac{1}{1 + A_{\Delta P,x\%}} \tag{16}$$

In addition to the previous indicators, the average PV energy curtailed $\overline{W}_{\mathrm{PV,cur}}^{(k)}$ is calculated from the $m = 1, \ldots, M^*$ occurrences $\overline{W}_{\mathrm{PV,cur},m}^{(k)}$ of PV energy curtailed:

$$\overline{W}_{\mathrm{PV,cur}}^{(k)} = \frac{1}{M}\sum_{m=1}^{M} W_{\mathrm{PV,cur},m}^{(k)} \tag{17}$$

2.4. Categorization of the PV systems and EV charging stations in the distribution system

The context of the application is grid-to-vehicle, in which the EVs need to be charged. The main goal is to address the issues regarding the energy curtailment of PVs installed in the grid, without adopting controlling strategies to enhance the operation of PV systems and without

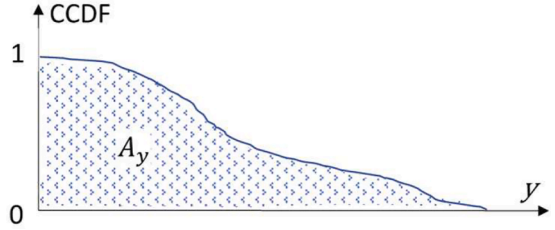

Fig. 1. Definition of the area from the CCDF.

the installation of BESS. In fact, the proposed method investigates on the capacity of EV batteries connected to the grid and through a charging power management of EV chargers mitigates the PV energy curtailments in a decentralized, secure, and traceable way. The distribution network considered is typically at the medium voltage level, considering that the EV charging infrastructure has to manage a sufficient number of EVs to guarantee the support needed to reduce the PV power curtailment to a significant extent.

The presence and location of PV systems and EV charging stations in the distribution network have an impact on the results of the power flow analysis. The EV charging strategy will be mostly influenced by the information on the PV systems located closer to the EV charging stations. For this purpose, information on the electrical distance among PV systems and EV charging stations is calculated and used in the definition of the EV charging strategy. In the radial network, the electrical distance is approximated by the absolute value of the sum of the series impedances found along the path between the nodes where the PV system and the EV charging station are located. The PV systems and EV charging stations are then grouped by using the kmeans clustering technique, using the electrical distances as features [55]. The initial number of clusters is chosen equal to the number of charging stations. However, based on the electrical distances, kmeans could assign more charging points to the same cluster, leaving other clusters without charging stations. The final number of clusters C considered is equal to the number of clusters formed by kmeans that contain at least one EV charging station (the other clusters are discarded). The PV systems located outside the C final clusters will not be taken into account to affect the EV charging strategy.

3. Framework for assessing PV power curtailment smart charging of electric vehicles with fuzzy weights and blockchain-based ev selection

3.1. Smart charging principles

The analysis is carried out by considering $i = 1, \ldots, I$ successive time steps with equal duration. In the three-phase system, it is also necessary to identify the phase $p = \{a,b,c\}$ to which the EV is connected in the charging station. The EVs $j = 1, \ldots, J$ are associated to the cluster $c = 1, \ldots, C$, to the charging station $n = 1, \ldots, N$, and to the plug $r = 1, \ldots, R_p$ at phase p to which each EV is connected.

The EVs connected to different points in the distribution system should meet three conditions so as to earn the allowance for increasing their charging power. These conditions are based on the following parameters:

1) the state of charge (SoC) of each EV
2) the loading percentage of the line; and,
3) the PV power production (indicated as RES in the sequel).

The proposed strategy is based on the generation of fuzzy weights, considering these parameters. The fuzzy weights are generated based on the "Mamdani fuzzy interference system" [56] and are assigned to each EV at each time step during charging. The three conditions are expressed in terms of fuzzy weights w_{ijcnpr} (detailed below) and of minimum PV power production $P^{\mathrm{PV,min}}$, as follows:

1) The fuzzy weight is higher than the average fuzzy weight $\overline{w}_{ijcnp}$ assigned to each plug located in the same charging station and connected to the same phase:

$$w_{ijcnpr} > \frac{\sum_{r=1}^{R} w_{ijcnpr}}{R} \tag{18}$$

2) The fuzzy weight is higher than the minimum value $w^{\min}$, with the objective of limiting the number of EVs that increase the charging power:

$$w_{ijcnpr} \geq w^{\min} \tag{19}$$

3) The PV power generation at the time step i is higher than the minimum limit, to exclude situations in which the generation from PV is very low:

$$P_i^{\mathrm{PV}} > P^{\mathrm{PV,min}} \tag{20}$$

where $P^{\mathrm{PV,min}} = \kappa^{\mathrm{PV}} P^{\mathrm{PV,peak}}$, in which κ^{PV} is a user-defined multiplier, and $P^{\mathrm{PV,peak}}$ is the per-phase peak power generation of each PV plant connected to the grid.

When these conditions are met, the proposed control strategy is activated to supply the eligible EVs. At each EV charging point, each phase has R plugs for EV charging. The increase in the EV charging power is not a fixed amount, since it fluctuates depending on the loading percentage of the lines that supply the charging stations, the PV production, and the SoC of each EV.

Fig. 2 illustrates the flow-chart that indicates the overall scheme of the calculations for different time steps. The availability of an excess of PV power production is checked in each cluster at each phase, to determine whether the EV charging can be increased. Fig. 3 shows the flow-chart of the internal calculation process at a given time step, cluster and phase. The calculation of the fuzzy weights (using the EV and grid parameters), the assignment of the fuzzy weights to the charging points (plugs) with EVs connected and the selection of the plugs in which the EV charging power has to be increased are included in the "smart contract" associated with the blockchain. The eligible plugs selected to increase the EV charging power, together with the output power, the type and identifier of the EV, the state of charge and the time stamp are the outputs of the "smart contract" that are added to the blockchain structure.

In more details, the control strategy monitors the amount of power injected by PV systems into the portion of the grid belonging to a cluster, in the corresponding phase p of the three-phase system and in the current time step i, and the power consumed in the previous time step i-1 in the same phase, and then calculates their difference. If the difference is positive, the excess power could be used by increasing loads, in our case by adding up the power of some chargers that feed the EVs in a coordinated manner. The procedure to increase the EV charging power for charging the selected EVs according to the selection mechanism previously explained is organized as follows (for simplicity of representation, the subscripts c, n and r are dropped off). The eligible EVs are allowed to increase their charging power P_{ijp}^{ch} up to the given power limit P_j^{lim} to protect EV batteries from damaging. In practice, the power to be increased at the $R_p^{'} \leq R_p$ chargers with eligible EVs connected at phase p is $\nu_p = P_p^{\mathrm{PV}} - P_{(i-1)p}^{\mathrm{load}}$, where $P_{(i-1)p}^{\mathrm{load}}$ stands for power consumed at the previous time step by all the loads including EVs connected to the grid:

- If $\nu_p > 0$, proportional sharing of the power to be increased is applied to the $R^{'}$ chargers, so that at each one of these chargers there is a power increase equal to $\nu_p / R^{'}$. If the power limit P_{jp}^{lim} is reached at any charger j connected to phase p, the power at that charger is limited to the power limit and the remaining chargers with eligible EVs will share the remaining power increase.
- If the condition $\nu_p > 0$ is not met, the EV charging power at phase p is not increased with respect to the situation already in place. This means that only in case of excess energy generation

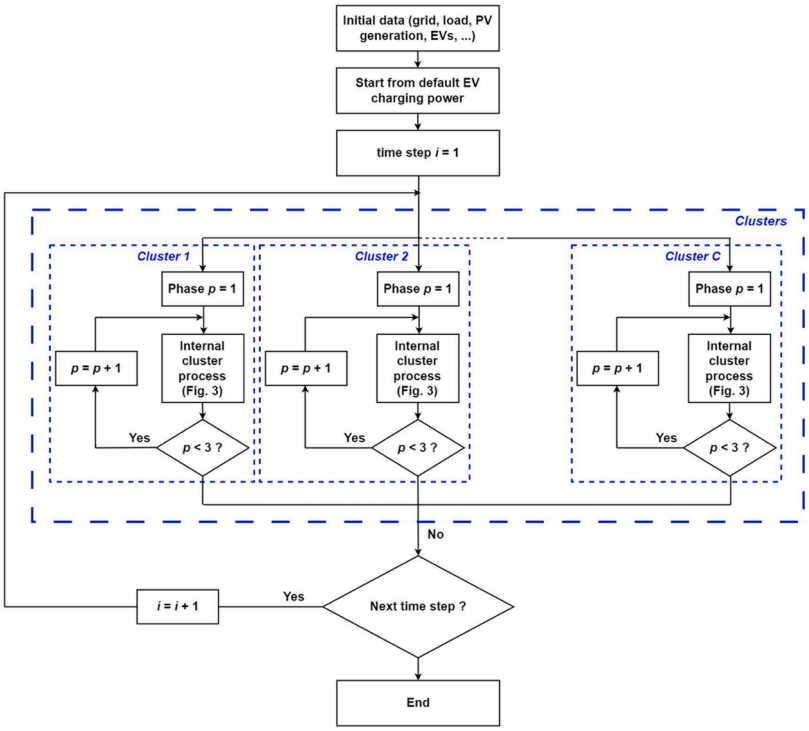

Fig. 2. Flow-chart of the overall scheme of the calculation process.

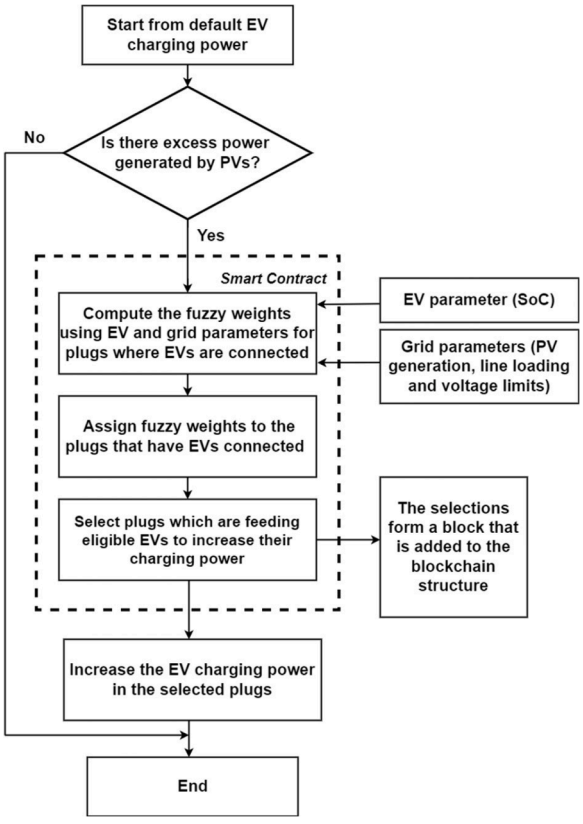

Fig. 3. Flow-chart of the internal calculation process at a given time step, cluster and phase.

by PVs the system would increase the charging power available to EVs.

3.2. *Fuzzy logic-based decision-making making*

The shape of the Membership Functions (MFs) depends on how one believes in a given linguistic variable. It is more a question of intuition than criteria. The only condition that a MF must really satisfy is that it must vary between 0 and 1. The function itself can be an arbitrary curve, whose shape can be defined as a suitable function from the point of view of simplicity, convenience, speed, and efficiency. Therefore, the type of MF does not play a crucial role in shaping how the model performs [57]. The intervals and number of MFs in this work are shaped intuitively and based on linguistic forms. Fig. 4 shows the MFs [58] used in the fuzzy logic model. The number of MFs belonging to each parameter is 3, 5, and 3, respectively.

In the definition of the MF for the per cent line loading, the maximum line loading considered is 90%, as a conservative limit to avoid the increase of the EV charging power when there are one or more lines too close to their limit. The fuzzy weights in the proposed methodology are generated phase by phase, and the per cent loading of the corresponding phase is considered as one of the three parameters for the generation of fuzzy weights at each phase (Fig. 5 shows the fuzzy logic-based decision-making unit diagram). In practice, if the line loading exceeds 90% at one phase of the grid, in the rules established the charging power of the EVs will not be changed in that phase.

The combinations of the MFs determine the overall number of rules which in this case is equal to 45. The decisions are made according to these rules, which are defined intuitively.

Some of the rules introduced are:

- If (SoC is low) and (RES is high-moderate) and (line loading is moderate) then (fuzzy weight is high)

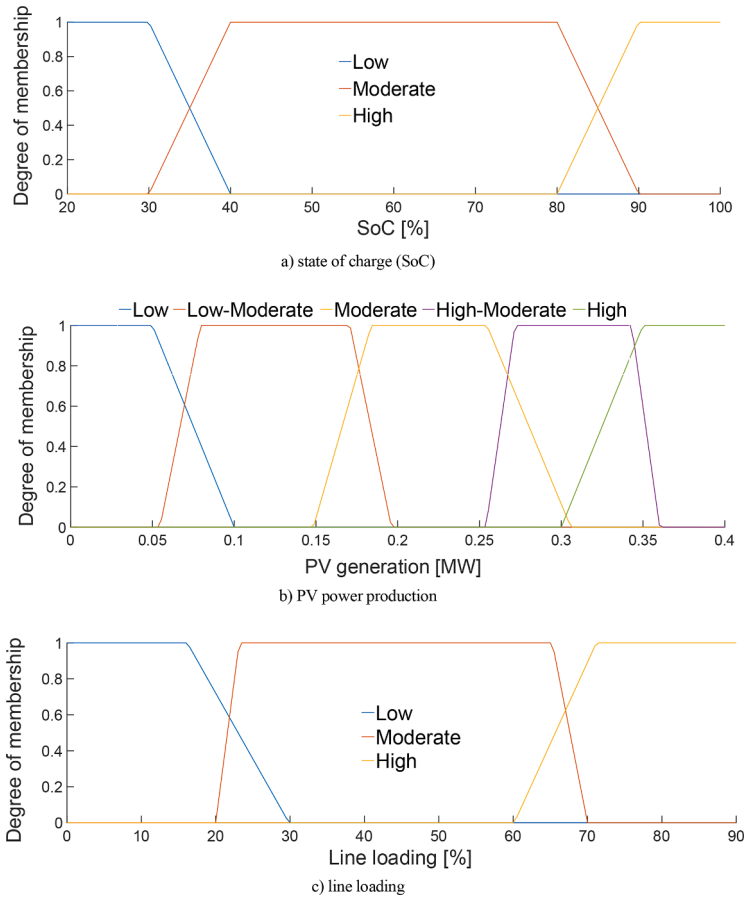

Fig. 4. Fuzzy membership functions for the input variables.

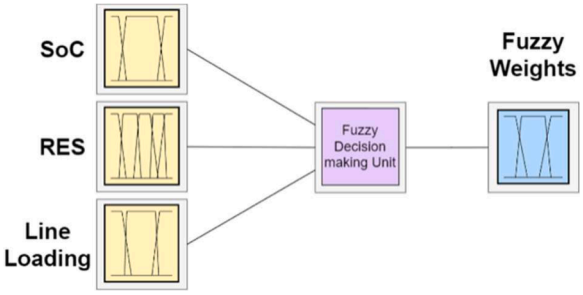

Fig. 5. Fuzzy logic decision-making diagram.

- If (SoC is moderate) and (RES is high) and (line loading is high) then (fuzzy weight is high)
- If (SoC is high) and (RES is high) and (line loading is low) then (fuzzy weight is medium)

The full set of fuzzy rules is provided in Section A of the Supplementary Material.

The strategy to define the fuzzy weights is backed up from the security point of view with adding up blockchain. At each time step, the transactions would be inserted inside blocks forged by the charging points to which EVs are connected (Fig. 6). The blockchain algorithms used in the charging strategy are incentive-based rather than stake-based [47]. The decentralization provided by blockchain ends up in omitting third parties to speed up the process and save energy and time

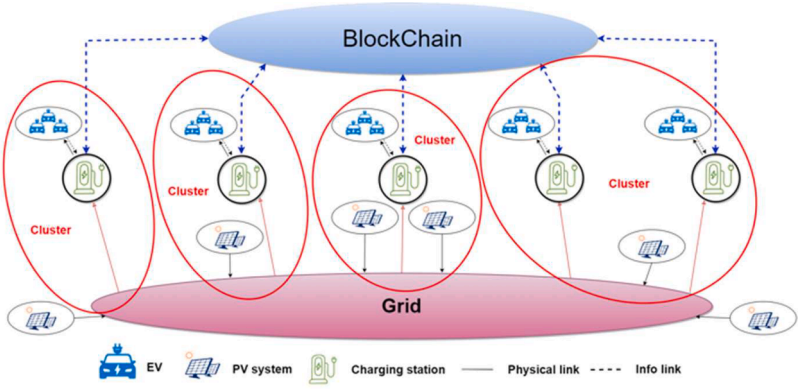

Fig. 6. Interconnections of the EV charging stations through blockchain.

as well. It is worth noting that the traceability feature of the blockchain is available here, so that the transactions done by EV charging plugs and the grid status can be monitored for further statistical studies.

3.3. Specific blockchain solution for decentralized and scalable EV charging infrastructure

The main benefits of adopting a blockchain-based solution in the management of EV charging infrastructures are the increased decentralization, security and scalability of the distribution network. In such scenario, charging data and transactions are not stored in a central system, but are distributed across a network of nodes, enhancing reliability, reducing risks of single-point-of-failure and making recharging infrastructure more robust [59]. Moreover, as the number of EVs and charging stations grows, the distributed nature of blockchain allows to easily scale up and to handle a large number of transactions efficiently, ensuring that the charging infrastructure can keep up with increasing recharging demand [60].

The proposed blockchain application is based on a PoA consensus protocol that selects the validator nodes by publishing the blocks (and thus the charging request transactions) on the blockchain based on their reputation and their identity, which is periodically validated. PoA is mainly adopted in private-permissioned blockchain approaches, and the advantages of using it include high security, scalability and lower energy consumption [61]. As shown in Fig. 7, the proposed solution leverages the fuzzy weights of the EVs connected to the same EV charging station and same phase of the network for the selection of the merit vehicles for increasing their charging power. In particular, if an EV that requests to increase its charging power has a fuzzy weight greater than the average of the fuzzy weights of all the other EVs involved in the charging phenomena at the same charging point (and the fuzzy weight is higher than the selected minimum threshold), the blockchain allows the vehicle to send a charging request transaction that will be validated and published by a pool of trusted validator nodes. Following the transaction, a permanent and immutable set of transaction data will be stored on the blockchain to guarantee full transparency and traceability of the recharging operations, as well as protection against malicious cyber-attacks (Fig. 7). The security aspect of blockchain would be reinforced over time as the number of members functioning to the network (in our case EVs connected to the charging station plugs) will be increased and it ends up in producing longer chains which are difficult to be manipulated by external attackers.

The Eqs. (11)–(13) determine the three sufficient conditions for the selection mechanism of EVs to increase their charging power: the EVs with fuzzy weights higher than the average of all fuzzy weights in the network and greater than the user-defined minimum would gain their profit in form of increasing their charging power. The node (charging plug) that has the greatest fuzzy weight among those chosen would forge the block containing the transactions into the chain.

4. Case study application to a distribution system

4.1. System data

The proposed method has been applied to a modified version of the IEEE 123-bus distribution network [62], supplied at the nominal voltage 4.16 kV. Since the original network provided in [63] has no PV and no EV charging points, PV systems have been added in specific nodes to simulate the impact of renewable energy on the whole grid. The configuration of the system is shown in Fig. 8. The PV generator locations have been chosen as in [64]. Single-phase PV inverters are connected to single-phase nodes at nodes 6, 11, 28, 43, 84, 90, 94, and 109. Three-phase PV inverters are connected to the three-phase nodes 48, 65, and 76. The PV system peak power generation at each phase of the interfaced inverters is 400 kW. The PV production data are extracted in both scenarios (sunny day and cloudy day) from one-minute data taken from real measurements in Southern Europe installations.

The load patterns are constructed based on one-minute load data of different types of users, taken from real measurements. The load data for the loads marked as PQ type in [63] have been aggregated to form different load patterns at each node, adding a number of individual load patterns in such a way that the peak power of the aggregate daily load pattern is comparable with the active power values indicated in the reference case for each phase of the IEEE 123-bus network. The load values for the other types of loads have not been changed. The evolution in time of the PQ loads at the specific nodes is provided in the Supplementary material.

The kmeans clustering algorithm based on the electrical distances has been executed as indicated in Section II.D, with 5 initial clusters (equal to the number of EV charging points). The nodes considered are the ones in which there are either PV generation or EV charging points. The electrical distances with respect to the charging points are summarized in Fig. 9. The electrical distances have been given to the clustering algorithm as inputs. The clustering results provide a vector in which each node is assigned the number of the cluster. In the clustering solution, two pairs of EV charging points have been grouped together, leading to $C = 3$ final clusters, as shown in Fig. 9.

The smart charging strategy has been evaluated with different number of charging plugs available in the grid, namely, 45, 90, and 135. This means that there are certain number of plugs designed in five charging stations located inside the grid and nine plugs per phase are provided by charging stations in the case with 135 plugs. The charging stations that feed the EVs are connected to the grid by means of MV/LV transformers at nodes 23, 44, 91, 105, and 610. The EV charging infrastructures are equipped with 7.4 kW and 22 kW chargers by default. The number of EVs connected to the grid, the specific brand of EVs, the

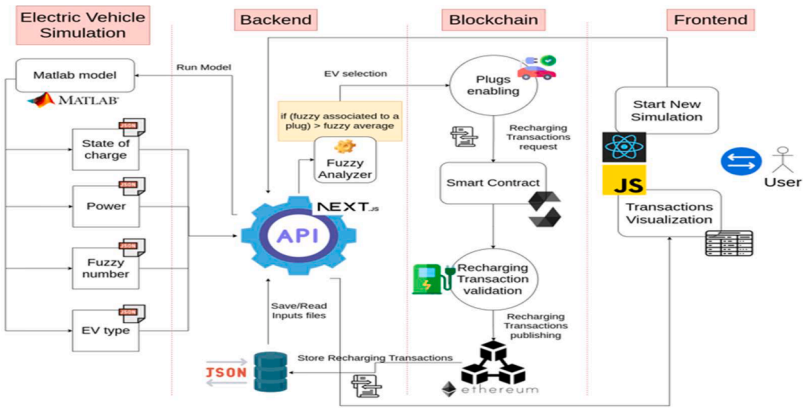

Fig. 7. Interactions among the computational models. The directions of the arrows indicate the information flow.

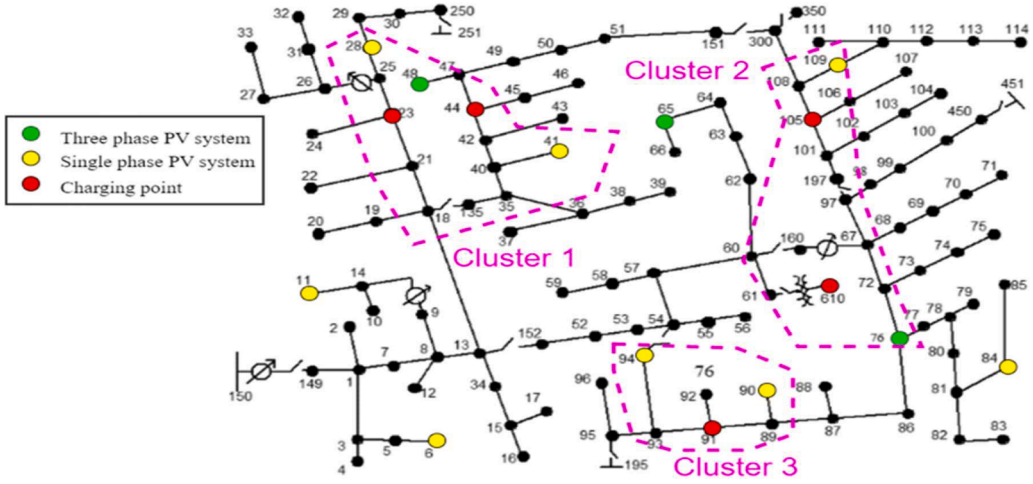

Fig. 8. IEEE 123-bus system (adapted). The lines from nodes 151–300 and 54–94 are open in the radial configuration analyzed.

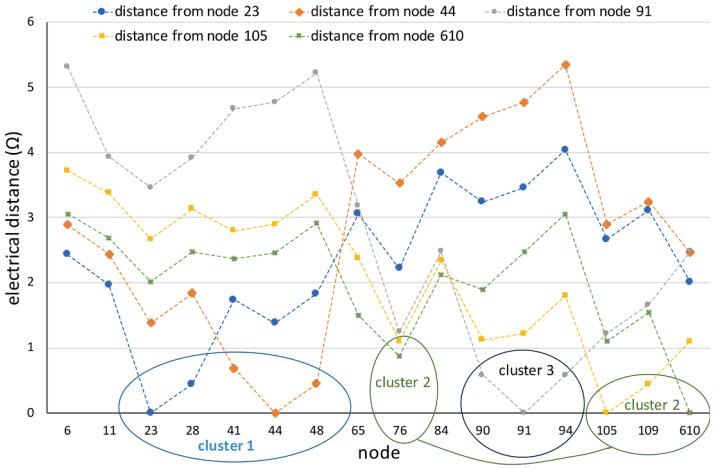

Fig. 9. IEEE 123-bus system (adapted). The lines from nodes 151–300 and 54–94 are open in the radial configuration analyzed.

type of charger they are using, the state of charge (SoC) of each EV, the duration for which each EV remains at the charging station with the arrival and departure times, all are selected randomly in a day. EVs are selected randomly among a group of five fully electric vehicles ("Dacia Spring", "Fiat 500E", "Smart EQ ForTwo", "Renault Twingo ZE", and "Renault Zoe"). The battery capacity of these EVs used in the simulations is chosen according to the brochures of the manufacturers. For picking up the random variables from a uniform probability distribution, it has been assumed that the EVs remain at the charging station with minimum of 30 min and maximum of 8 h, with the initial SoC selected between 20% and 95%.

The values considered for assigning the fuzzy weights (from Section 3.1) are $\kappa^{\mathrm{PV}} = 0.1$ and $w^{\min} = 0.5$.

4.2. Computational framework and results

The performance of the method proposed in this paper is assessed by considering two scenarios, one in a sunny day with clear sky and one in a cloudy day, with three case studies in each scenario. The first case is the reference case, with clear sky over the whole territory, which sets up the terms of comparison with the solutions of the other two cases that represent EVs connected to the grid in the uncoordinated or coordinated manners. The reference case is executed without imposing grid constraints and without EVs.

The peak PV power generation injected into the grid by the inverters in each phase in the reference case (sunny day) for every PV plant per phase is $P_{\mathrm{PV}}^{\mathrm{ref}} = 400$ kW at timestep #805, and the corresponding energy generated in the same day $W_{\mathrm{PV}}^{\mathrm{ref}} = 3.256$ MWh.

According to network analysis, the application of the proposed charging strategy to mitigate PV energy curtailment has no negative impact on the voltage profile of the buses, as there is no over-voltage or under-voltage in the grid. The voltage magnitudes remain always in the range from 0.9 to 1.1 per unit. Based on the simulations carried out, the overloads occur in the lines close to the supply point, which connect the nodes 149, 1, 7, 8, and 13.

The PV energy curtailment mitigation results from the integration of the smart charging strategy for EVs into the charging stations. The best solution would have no PV energy curtailment during specific times of a day thanks to the augmented charging power of the eligible EVs selected.

4.2.1. First scenario (Sunny day)

The PV data are taken from a summer day in Italy, where during the summer there is a shift of one hour, so that the peak power in a sunny

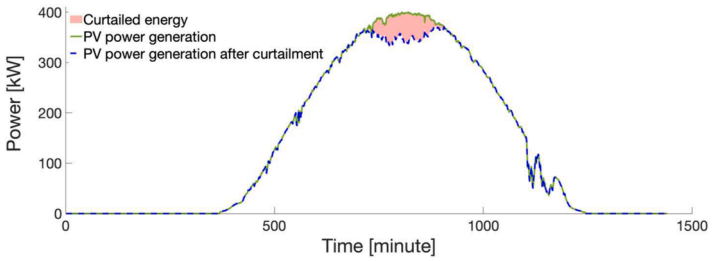

Fig. 10. PV power generation with uncoordinated EV charging (sunny day).

day is expected to occur at 1 pm. The results of two cases with uncoordinated EV charging and coordinated EV charging (the latter, labelled with "after", applies the proposed methodology) indicate that:

a) For EVs connected to the grid in an uncoordinated manner ($k = 1$): the peak power generation of each PV system per phase is $P_{\mathrm{PV}}^{(1)} = 371.5$ kW at timestep #886, which ends up in the peak power curtailment $P_{\mathrm{PV,cur}}^{(1)} = 63.6$ kW. The total energy generated is $W_{\mathrm{PV}}^{(1)} = 3.147$ MWh and the corresponding energy curtailment is $W_{\mathrm{PV,cur}}^{(1)} = 109.4$ kWh.
b) For EVs connected to the grid in the coordinated manner ($k = 2$): the PV peak power generation in this case is $P_{\mathrm{PV}}^{(2)} = 400$ kW at timestep #805, with null peak power curtailment. Figs. 10 and 11 depict the PV energy curtailment with and without the EV charging strategy per phase, and the colored area indicates the PV energy curtailed. In both cases, simulations are carried out with the same number of EVs connected to the grid in the coordinated and uncoordinated manners. The proposed method for EV charging manages the energy generated by PVs properly and prevents PV generation from being curtailed. The maximum PV power reduction in Fig. 10 (equal to 62.6 kW) occurs at time step #812. The maximum PV power reduction in Fig. 11 is null.

Fig. 12 shows the results achieved in the presence of EVs connected to the grid randomly, without and after the implementation of the EV controlling strategy in the grid-to-vehicle mode. To guarantee comparability, the simulations have been executed by using the same initial seed for random number extraction. The per cent maximum loading is 99.6% and occurs at phase "a" at time step #781.

The results of the EV charging at a grid node are presented in the Appendix.

4.2.2. Second scenario (Cloudy day)

The same simulations have been carried out to evaluate the impact of the proposed methodology on PV energy curtailment in a cloudy day (again in the summer period in Italy). Basically, there could be some time periods in which the PV power is excessively high and would have to be curtailed in a cloudy day, so the EV charging strategy can be effective in mitigating the PV power curtailment in these time periods. The peak power produced by each PV system is $P_{\mathrm{PV}}^{\mathrm{ref}} = 400$ kW at timestep #847. The total PV energy produced during the day from all PV systems is $W_{\mathrm{PV}}^{\mathrm{ref}} = 2.6167$ MWh.

The two cases studied are:

a) EVs connected to the grid in an uncoordinated manner ($k = 3$): the peak PV power generation occurs at timestep #831, and it is equal to $P_{PV}^{1} = 371.7$ kW and the corresponding peak power curtailment is $P_{\mathrm{PV,cur}}^{(3)} = 55.66$ kW, the energy injected to the grid is $W_{\mathrm{PV}}^{(3)} = 2.5784$ MWh, and $W_{\mathrm{PV,cur}}^{(3)} = 38.3$ kWh has been curtailed.
b) EVs connected to the grid in coordinated manner ($k = 4$): the peak PV power generation is$P_{\mathrm{PV}}^{(4)} = 396.4$ kW taking place at timestep #882 and leading to the peak power curtailment $P_{\mathrm{PV,cur}}^{(4)} = 25.06$ kW. The total energy production is $W_{\mathrm{PV}}^{(4)} = 2.6117$ MWh with the corresponding curtailed energy $W_{\mathrm{PV,cur}}^{(4)} = 5.0$ kWh.

Figs. 13 and 14 indicate the feasibility of the proposed methodology in a cloudy day. Also in this case, the proposed approach manages the PV energy production to mitigate the PV energy curtailment close to the PV production peaks. The smart charging system stores the excess PV energy into the EV batteries, decreasing the network branch loading as occurred in the first scenario (Fig. 15).

4.3. Effectiveness indicators under uncertainty

To consider the impact of uncertainties on the random variables referring to the EVs (at given PV generation), the indications of Section 2.3 have been followed. The details are shown below for two representative random variables, i.e. the PV energy curtailed $W_{\mathrm{PV,cur}}^{(k)}$ and the PV peak power reduction $\widehat{P}_{\mathrm{PV,red}}^{(k)}$. The Monte Carlo simulations have been executed by considering the stop criterion indicated in Eq. (11), considering the 99% confidence bounds correspond to $\alpha = 0.01$ and $z_{\alpha/2} = 2.58$, and with different thresholds $\varepsilon_{\mathrm{MC}}$. Common value used in the literature are $\varepsilon_{\mathrm{MC}} = 0.05$ or $\varepsilon_{\mathrm{MC}} = 0.01$. The minimum and maximum numbers of Monte Carlo simulations executed have been equal to 10 and 400, respectively. In the cases tested, the results have been particularly positive, so that it has been necessary to reduce the thresholds to remarkably low values to find values higher than 10 of the minimum number of Monte Carlo simulations M_{MC} needed to obtain a Monte Carlo test error lower than the threshold $\varepsilon_{\mathrm{MC}}$. Table 1 shows the values of M_{MC} obtained for different thresholds $\varepsilon_{\mathrm{MC}}$. From the results shown in Table 1, it emerges that M_{MC} is significantly lower for the PV energy curtailment with respect to the PV peak power reduction. This can be explained by the variability of the location of the peak power reduction in the different cases, which makes the solutions more variable. Moreover, concerning the cases analyzed, the EV coordinated cases show higher M_{MC} values than the EV uncoordinated cases, because in the coordinated cases there are the effects of the smart charging strategies, that lead to more variable EV charging patterns with respect to the regular EV charging carried out in the EV uncoordinated case. Finally, in the cloudy day cases the M_{MC} values are lower than in the sunny days for the PV

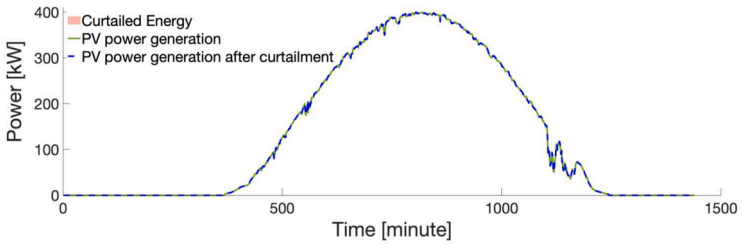

Fig. 11. PV power generation with coordinated EV charging (sunny day).

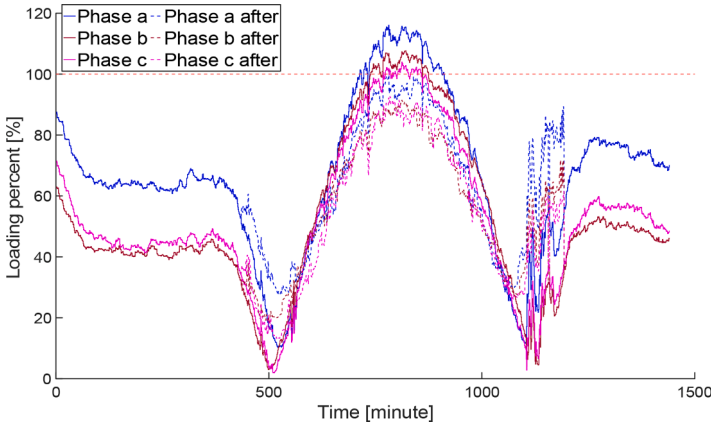

Fig. 12. Loading of the three phases of line between nodes 149 and 1 without and after considering the coordinated EV charging (sunny day).

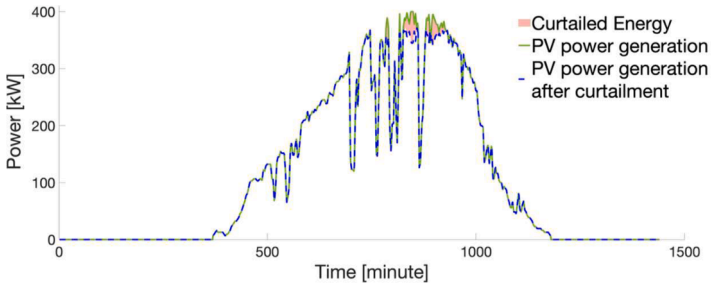

Fig. 13. PV power generation with uncoordinated EV charging (cloudy day).

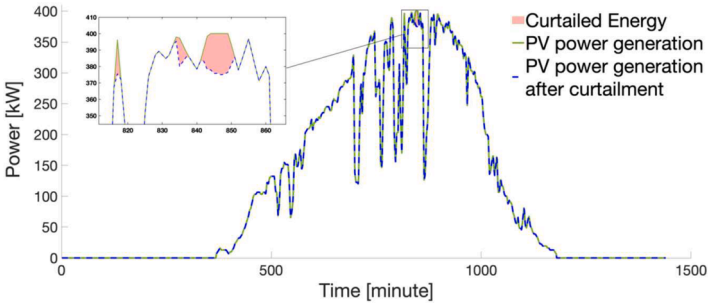

Fig. 14. PV power generation with coordinated EV charging (cloudy day).

energy curtailment, as there is a smaller period in which the curtailment appears, while the M_{MC} values are higher than in the sunny days for the PV peak power reduction, because of the variability of the peaks due to less regular PV power production during time. The same comments are valid for the contents shown in Table 2, in which the variation of the Monte Carlo test error is shown for different numbers of simulations, indicating a converging trend in all cases. Furthermore, Table 3 shows how the Monte Carlo test error changes in two successive numbers of simulations. From the plots shown in Table 3 emerges that the changes are remarkably small already after a few dozens of iterations.

Based on the results obtained, the number M^* =100 Monte Carlo simulations is chosen for calculating the effectiveness indicators reported in Section 2.3, in such a way to have a common value for all calculations, which is also large enough to form the CCDFs with an acceptable number of points. The simulation time to determine the sharing of the PV power between the plugs where EVs are connected in a single Monte Carlo simulation executed on the entire day on a 11th Gen Intel® Core™ i7–1165G7 @ 2.80 GHz laptop has been about 20 s for a

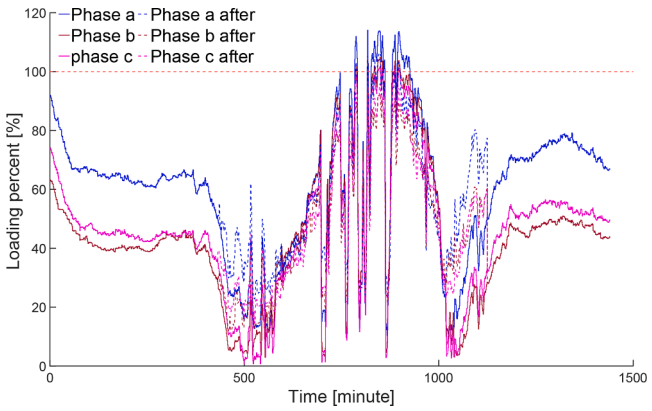

Fig. 15. Loading of the three phases of line between nodes 149 and 1 before and after considering the coordinated EV charging (cloudy day).

sunny day, while it has been lower for cloudy days in which there are less time steps in which the EV charging power has to be increased.

The minute-by-minute simulations throughout a day executed $M^* = 100$ times have then been considered, and the effectiveness indicators in the EV uncoordinated and coordinated charging cases have been calculated. Considering the sunny day, the CDF of the PV energy produced is indicated in Fig. 16, and the CCDF of the PV energy curtailed is shown in Fig. 17. The results end up in *avoided PV energy curtailment effectiveness* $\xi_W^{(1)} = 0.969$ for the EV uncoordinated charging case, which increases to $\xi_W^{(1)} = 0.992$ in the EV coordinated charging case. The average PV energy curtailed is $\overline{W}_{\mathrm{PV,cur}}^{(1)} = 102.9$ kWh in the EV uncoordinated charging case and $\overline{W}_{\mathrm{PV,cur}}^{(2)} = 25.7$ kWh in the EV coordinated charging case.

Considering the PV peak power, the CDF is shown in Fig. 18, while Fig. 19 reports the CCDF of the PV peak power reduction. The *PV peak power reduction effectiveness* is $\xi_{\Delta\hat{P}}^{(1)} = 0.938$ in the EV uncoordinated case and becomes $\xi_{\Delta\hat{P}}^{(2)} = 0.993$ in the EV coordinated case. The PV power reduction effectiveness at 5% is $\xi_{\Delta P,5\ \%}^{(1)} = 0.872$ in the EV uncoordinated case and $\xi_{\Delta P,5\ \%}^{(2)} = 0.931$ in the EV coordinated case.

Table 4 shows the effectiveness indicators in the cloudy day. The benefits of applying the coordinated EV strategy are still evident, even if these benefits are less due to shorter periods that would require a reduction in the PV production.

4.4. Comparisons with another EV charging management system

An emblematic method to be compared with the proposed approach is presented in Ref. [23]. This method proposes a charging control

Table 1
Minimum number M_{MC} of Monte Carlo simulations for different thresholds $\varepsilon_{\mathrm{MC}}$. The superscripts indicate the cases analyzed, with (s,u): sunny day, EV uncoordinated; (s,c): sunny day, EV coordinated; (c,u): cloudy day, EV uncoordinated; and (c,c): cloudy day, EV coordinated.

$\varepsilon_{\mathrm{MC}}$	random variable							
	$W_{\mathrm{PV,cur}}^{(\mathrm{s,u})}$	$\widehat{P}_{\mathrm{PV,red}}^{(\mathrm{s,u})}$	$W_{\mathrm{PV,cur}}^{(\mathrm{s,c})}$	$\widehat{P}_{\mathrm{PV,red}}^{(\mathrm{s,c})}$	$W_{\mathrm{PV,cur}}^{(\mathrm{c,u})}$	$\widehat{P}_{\mathrm{PV,red}}^{(\mathrm{c,u})}$	$W_{\mathrm{PV,cur}}^{(\mathrm{c,c})}$	$\widehat{P}_{\mathrm{PV,red}}^{(\mathrm{c,c})}$
0.001	63	>400	187	>400	12	>400	52	>400
0.002	19	47	46	119	<10	37	18	217
0.003	<10	23	23	31	<10	18	<10	66
0.004	<10	12	<10	<10	<10	13	<10	41
0.005	<10	<10	<10	<10	<10	<10	<10	27

Table 2
Monte Carlo test error for increasing number of simulations.

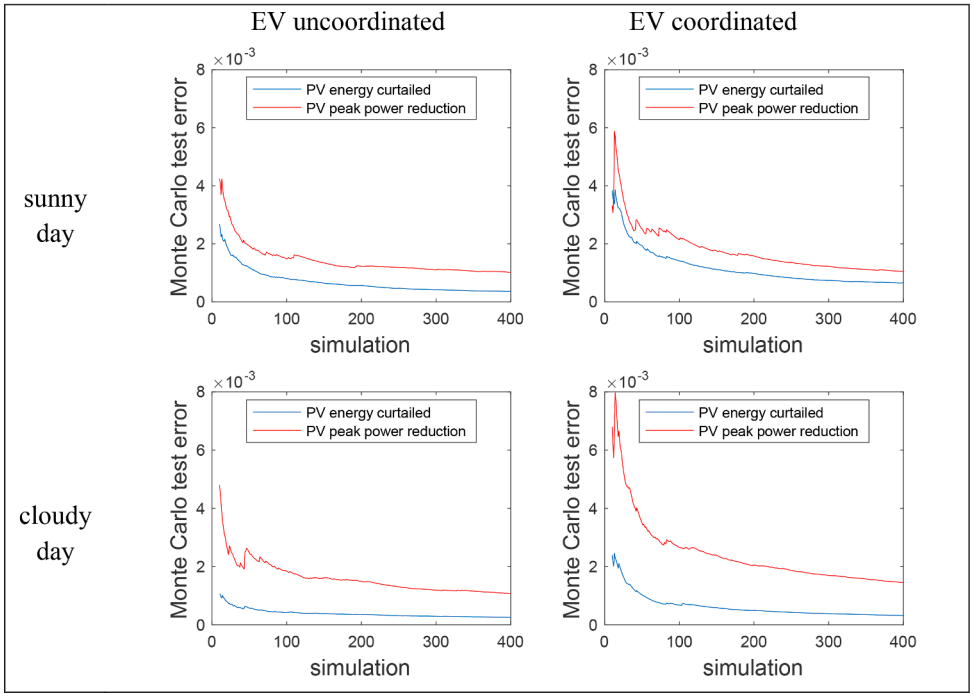

Table 3
Variation of the Monte Carlo test error at two successive numbers of simulations.

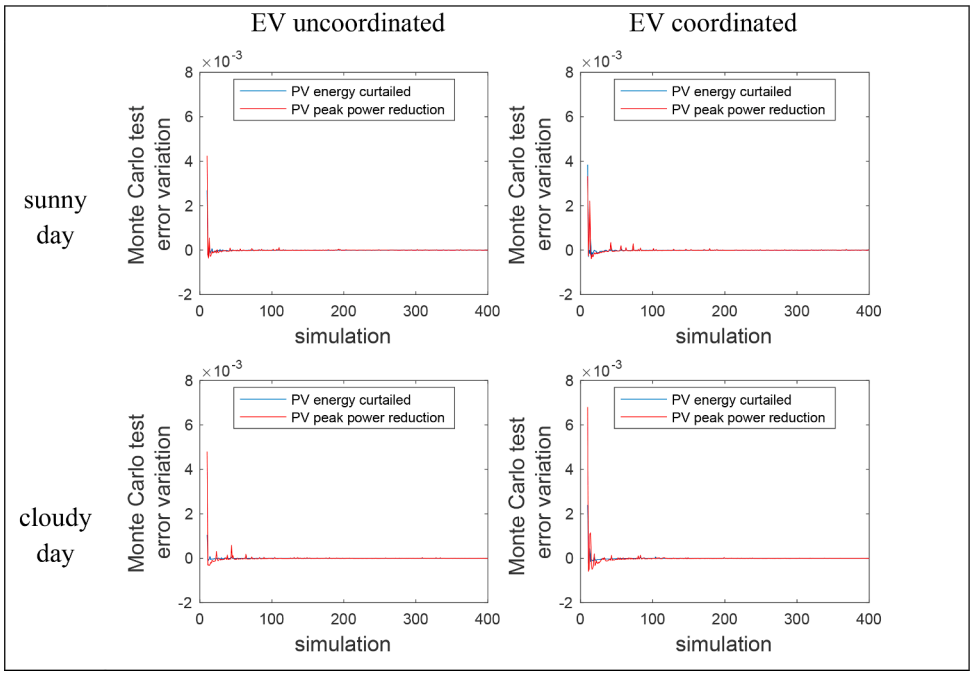

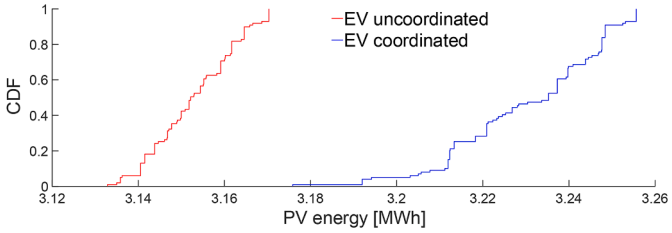

Fig. 16. PV energy produced in the sunny day.

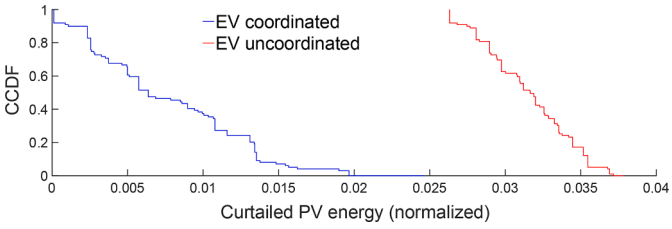

Fig. 17. PV energy curtailed in the sunny day.

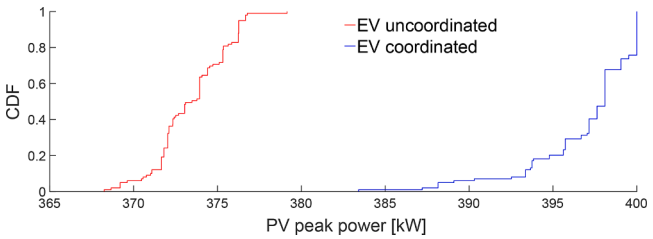

Fig. 18. PV peak power in the sunny day.

system based on the vehicle-to-grid (V2G) configuration to mitigate the PV generation curtailment during the peak power production hours. EV aggregators manage the charging and discharging of the EVs connected to the charging points. The method follows the principle of valley filling

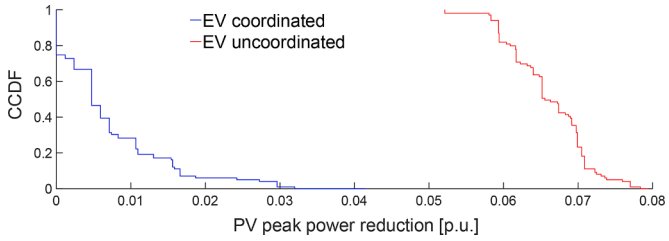

Fig. 19. PV peak power reduction in the sunny day.

Table 4
Effectiveness indicators in the cloudy day.

Case	$\overline{W}_{\mathrm{PV,cur}}$	ξ_W	$\xi_{\Delta\hat{P}}$	$\xi_{\Delta P,5\%}$
EV uncoordinated	37.5 kWh	0.828	0.939	0.874
EV coordinated	8.7 kWh	0.834	0.987	0.924

for mitigating the excess PV power generation that is injected into the grid. The valley-filling problem is formulated in Ref. [23] considering a set of scenarios with the corresponding weighting probabilities. For the sake of comparison with the results shown in the proposed approach, in which there are two scenarios (sunny day and cloudy day) the results are presented separately for the two scenarios.

The objective function considered for each scenario is:

$$\min\left\{\sum_t \left(L_{\mathrm{target},t} - D_t - P_t^c + P_t^d\right)\right\} \tag{21}$$

Table 5
Effectiveness indicators in the sunny day from hourly-based analysis.

Case	$\overline{W}_{\mathrm{PV,cur}}$	ξ_W	$\xi_{\Delta\hat{P}}$	$\xi_{\Delta P,5\%}$
EV coordinated	67.2 kWh	0.980	0.964	0.946
From Ref. [23]	130.2 kWh	0.961	0.930	0.886
EV uncoordinated	142.0 kWh	0.958	0.924	0.878

where, at time step t, L_{target} is the target total generation without PV power curtailment, D_t is the total demand, while P_t^c and P_t^d represent the EV charging and discharging power, respectively, under the constraint that charging and discharging cannot occur at the same time.

Hourly time steps are used in Ref. [23] and are considered here in the comparison with the proposed approach. The simulations have been executed with 100 Monte Carlo repetitions for taking into account the impact of uncertainties on the random variables referring to the EVs, with the same type of calculations carried out in Section 4.3. The two cases (EV uncoordinated and EV coordinated) have been compared with the results obtained by applying the procedure presented in Ref. [23]. The indicators reported in Section 2.3 have been used to provide a comparison based on a global assessment of the results obtained. These indicators are shown in Table 5 for a sunny day and in Table 6 for a cloudy day. In all the cases shown, the proposed approach in the EV coordinated case shows better results than the ones obtained by applying the method of Ref. [23], with lower values of the energy curtailed $\overline{W}_{\text{PV,cur}}$ and higher values of the effectiveness indicators ξ_W, $\xi_{\Delta\bar{P}}$, and $\xi_{\Delta P,5\ \%}$. In turn, the result obtained in the EV uncoordinated case are worse than in the other two cases.

For the sunny day, the CDF of the PV energy produced is indicated in Fig. 20, and the CCDF of the PV energy curtailed is shown in Fig. 21. The total PV energy generated, calculated from hourly values, is 3.256 MWh. The PV energy in the solution proposed in this paper is 3.189 MWh, with 67.2 kWh of PV energy curtailment. Moreover, for uncoordinated charging the PV energy is 3.114 MWh, with 142.0 kWh of PV energy curtailment. With the methodology presented in Ref. [23], the PV generation is 3.126 MWh, with 130.2 kWh of PV energy curtailment. From the detailed results provided in the method presented in Ref. [23], it appears that even though V2G is allowed by the method, there is no contribution of V2G in the period corresponding to PV power curtailment, namely, all the EVs are operated in the grid-to-vehicle mode in that period. This is clearly explainable, as in the period of high PV production, when PV power curtailment could be more likely, in the presence of power injections in the grid from V2G, the situation would become worse, requiring more PV power curtailment. This aspect is also evident by looking at Eq. (14), where setting to zero the terms P_t^d at the various time steps contributes to reaching the minimum of the objective function, confirming the validity of the proposed approach based on grid-to-vehicle charging of EVs. Fig. 22 shows an example of PV power generation for one of the repetitions, showing the PV power reductions needed in the various situations with respect to the reference (unrestricted) case with no PV power curtailment.

The comparisons with respect to the peak power are not shown, as the determination of the peak power based on hourly data is poorly significant with respect to the actual evolution of the power patterns [65].

For the cloudy day, the CDF of the PV energy produced is indicated in Fig. 23, and the CCDF of the PV energy curtailed is shown in Fig. 24. The total PV energy generated, calculated from hourly values, is 2.688 MWh. The PV energy in the solution proposed in this paper is 2.681 MWh, with 7.1 kWh of PV energy curtailment. Moreover, for uncoordinated charging the PV energy is 2.631 MWh, with 56.7 kWh of PV energy curtailment. With the methodology presented in Ref. [23], the PV generation is 2.639 MWh, with 49.2 kWh of PV energy curtailment. Also in this case, in the period corresponding to PV power curtailment there is no contribution of V2G, and all the EVs are operated in the grid-to-vehicle mode. Fig. 25 shows an example of PV power generation for one of the repetitions in a cloudy day, indicating the PV power reductions needed in the various situations with respect to the reference (unrestricted) case with no PV power curtailment.

The results of the various comparisons executed clearly show that the proposed approach performs considerably better than the method defined in Ref. [23].

Table 6
Effectiveness Indicators in the cloudy day from hourly-based analysis.

Case	$\overline{W}_{\text{PV,cur}}$	ξ_W	$\xi_{\Delta\bar{P}}$	$\xi_{\Delta P,5\%}$
EV coordinated	7.1 kWh	0.849	0.961	0.987
From Ref. [23]	49.2 kWh	0.839	0.917	0.932
EV uncoordinated	56.7 kWh	0.838	0.907	0.927

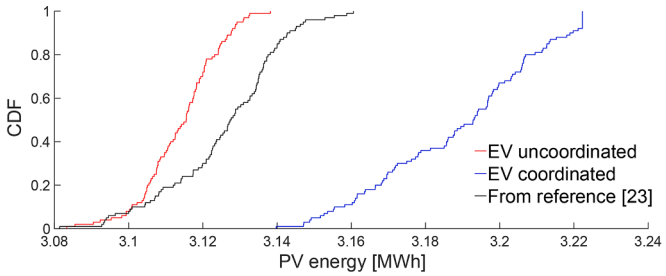

Fig. 20. Comparison among the CDFs of the PV energy produced in the sunny day (hourly data).

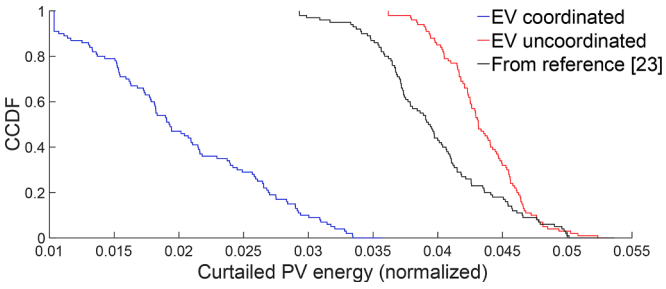

Fig. 21. Comparisons among the CCDFs of the PV energy curtailed in the sunny day (hourly data).

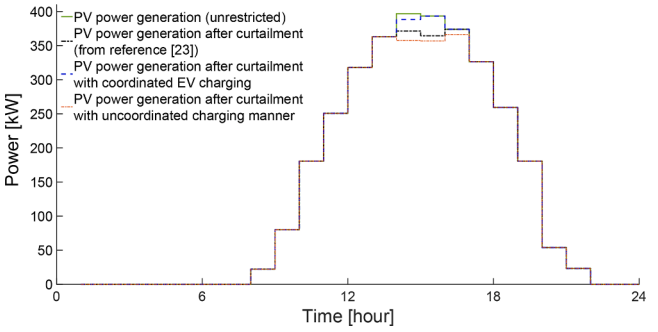

Fig. 22. PV power generation in the sunny day (hourly data).

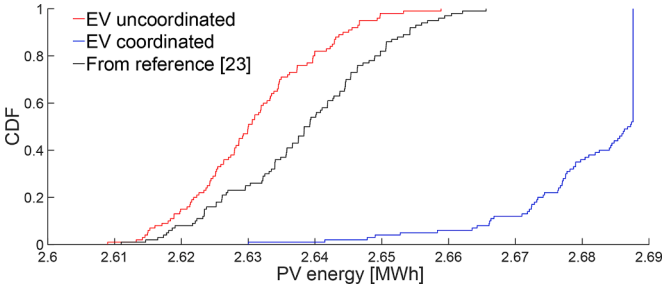

Fig. 23. Comparison among the CDFs of the PV energy produced in the cloudy day (hourly data).

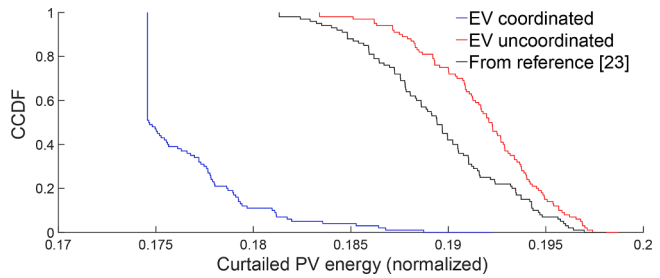

Fig. 24. Comparisons among the CCDFs of the PV energy curtailed in the cloudy day (hourly data).

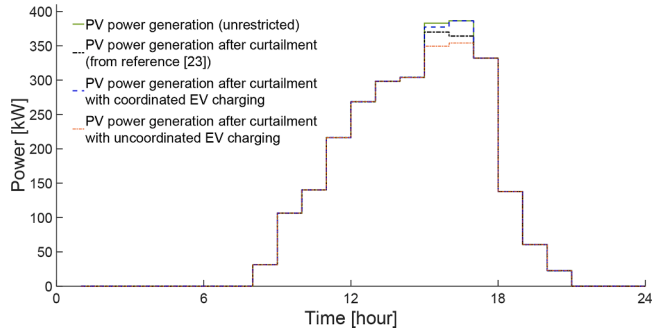

Fig. 25. PV power generation in the cloudy day (hourly data).

5. Concluding remarks

A novel dedicated framework for characterizing the PV generation curtailment in the grid has been presented, proposing new indicators to assess the effectiveness of solutions for mitigating the PV power and energy curtailment. Within this framework, the smart charging of EVs has been considered as a viable solution for grid-to-vehicle applications. An EV smart charging strategy has been proposed, in which the EVs are supplied by the excess energy produced by the PV system, and the EV charging power is managed through a strategy based on fuzzy weights, backed up by blockchain to guarantee security in the selection of the charging points, considering the variation of the EV charging power as a transaction.

The mitigation of the PV energy curtailment depends on the number and characteristics of the EVs connected to the grid. To consider the impact of the EV charging stations as an additional load that can be locally balanced with more PV generation, a clustering procedure has been executed to group the EV charging stations with some PV systems based on the electrical distance. In this way, the assignment of fuzzy weights to the charging points in the EV charging stations is driven by the PV generation located in the same cluster.

In particular cases, where a cluster contains no PV system, the fuzzy weights in the EV charging points belonging to that cluster are inactive, and the charging of the corresponding EVs occurs as in the uncoordinated charging case. However, in the future evolution of the grid, new PV systems and EV charging points are (very) likely to become available, and the update of the clustering algorithm will take into account the new situation. In this regard, the results of the clustering procedure and the indicators determined can disclose useful information about the effectiveness of the location of the PV system and EV charging stations in the grid.

The results obtained indicate the higher effectiveness of using the proposed coordinated strategy for EV charging with respect to the uncoordinated case, considering realistic random variations for the number of the EVs present in the EV charging stations, as well as their technical characteristics and timings of arrival and departure. The effectiveness of the proposed methodology has been evaluated in two different case scenarios: sunny day and cloudy day. The results clearly indicate that the implemented method could be effective in mitigating PV generation curtailments even in cloudy days when the continuity of energy production is not guaranteed, and the power production curve consists of many fluctuations. Running Monte Carlo simulations, the uncertainties are evaluated since the number of EVs connected to the grid varies throughout a day and the figures depict the effectiveness of coordinated charging manner proposed in this paper in comparison with uncoordinated charging manner where EVs are connected to the grid randomly and are immediately charged after their arrival. The proposed approach is transparent to the user, as it provides full information about the eligible EVs chosen to store the excess amount of PV energy during time. The requests of each EV user (i.e. to have the EV charged at the minimum desired state of charge at the end of the permanence period in the charging station) are in any case satisfied in the proposed methodology with or without the user's participation in the smart charging.

In the comparison with another method proposed in the literature, which also considers V2G, executed by considering uncertainties and assessed through the global indicators of effectiveness, the proposed approach in the EV coordinated charging mode performs better than the approach proposed in Ref. [23], while the cases with EV management in the uncoordinated charging mode are worse, confirming that the practices that include EV coordination are effective to reduce PV energy curtailment in the periods of high PV power production.

The proposed approach can be used with any type of generation, load of storage connected to the local distribution network. The inclusion of private blockchain, based on the PoA consensus algorithm in the charging procedure of the EVs not only guarantees the security of the network against malicious tampering of information, but also provides decentralization and traceability features, with EVs reaching the consensus among themselves without the intervention of third parties. This ends up in the reduction of time and costs for the EV charging management. The status of EVs and grid may be traced and monitored in every moment thanks to the ambient provided the distributed ledger tech.

The limitations of the proposed approach could come from its application in real-world situations, as the outcomes concerning the EVs depend on the forecast values of loads and of PV generations. This limitation is common to any approach that must be applied in real conditions. A positive aspect in this respect is that the largest energy curtailment occurs in sunny days, in which the PV power generation during time can also be more predictable, so that the real-case solutions should be considerably similar from the simulated solutions. Another limitation is that the proposed method depends on the number of EVs connected to the grid. If the number of EVs connected to the grid is not large enough when the EV support is needed (especially during the PV peak power generation in a sunny day), the PV energy curtailment mitigation could not be guaranteed due to the lack of additional load available from the EV side. Likewise, if there is a failure in the electronic boards or communication system for one or more EVs and their charging stations, the contribution of these EVs cannot be considered by the charging management system.

CRediT authorship contribution statement

Soheil Saadatmandi: Conceptualization, Data curation, Methodology, Software, Validation, Writing – original draft, Writing – review & editing. **Gianfranco Chicco:** Conceptualization, Data curation, Methodology, Software, Supervision, Validation, Writing – original draft, Writing – review & editing. **Alfredo Favenza:** Conceptualization, Methodology, Writing – original draft, Writing – review & editing. **Alessandro Mozzato:** Conceptualization, Methodology, Software, Validation, Writing – review & editing. **Francesco Giordano:** Conceptualization, Methodology, Writing – original draft, Writing – review & editing. **Maurizio Arnone:** Conceptualization, Methodology, Writing – review & editing.

Declaration of competing interest

The authors declare the following financial interests/personal relationships which may be considered as potential competing interests:

Soheil Saadatmandi reports financial support was provided by Government of Italy Ministry of Education University and Research.

Data availability

Data will be made available on request.

Acknowledgment

The first author acknowledges the PhD grant DOT1332092-7 received in application of the Italian Ministry Decree DM 1061/2021.

Supplementary materials

Supplementary material associated with this article can be found, in the online version, at doi:10.1016/j.epsr.2024.110181.

Appendix

Results of EV charging at a grid node

To show some details on the fuzzy weights and their impact on the selection of the plugs with EVs connected to activate, let us consider the three phases of node #23, connected to cluster #1, for the time steps from minute 400 to minute 1000. In particular, there are three plugs (identified as $r =$ 19, 20, and 21) at phase "a", three plugs ($r = 22$, 23, and 24) at phase "b", and three plugs ($r = 25$, 26, and 27) at phase "c". The EVs connected to the plugs are identified by their EV type and associated individual identifier. With reference to the indications provided in Section 3.1, Fig. A1 reports the fuzzy weights associated with the plugs at the three phases and Fig. A2 shows the SoC of the EV batteries for the EVs connected, compared with the EV uncoordinated case. The results indicate that at minute 600 there are 1 EV connected to a plug at phase "a" (#20) and 2 EVs connected to two plugs at phase "c" (#26 and #27). The EV batteries connected to all these plugs already reached their maximum SoC and cannot be used for further SoC increase until the EV leaves the plug and another EV arrives. In the period from minute 400 to minute 1000, the EVs connected to the plugs #26 and #27 are never selected by the EV coordinated charging strategy, as the batteries of the corresponding EVs have already reached the maximum SoC and the EVs remain connected for the whole period.

At minute 605 an EV is connected to plug #23 and is selected in the coordinated EV charging strategy to increase the charging power immediately (and the fuzzy weight is assigned), while in the uncoordinated EV charging strategy this EV would be charged at the default charging power (Fig. A2). In the EV coordinated charging strategy, this EV reaches the maximum SoC at minute 616, then its fuzzy weight remains high because the PV generation and load conditions would require more EV load, however, this plug will not be selected anymore.

At minute 611 the EV connected to plug #20 leaves after having reached its maximum time to remain connected, and another EV arrives and is connected to the plug. At this time step, in the EV coordinated charging strategy there are the conditions to increase the EV charging power immediately (as shown in Fig. A1 by the assignment of the fuzzy weight), while in the EV uncoordinated strategy this EV would be charged at the default charging power).

At minute 625 there is a reduction of the fuzzy weight for plug #20; however, plug #20 continues to be selected for charging until the battery of the EV connected reaches the maximum SoC (at minute 631). In the successive time steps, fuzzy weights are still assigned to plug #20, however, this plug is not selected anymore.

At plug #25, an EV arrives at minute 637 and is immediately assigned a high fuzzy weight, however, plug #25 is not selected by the EV coordinated charging strategy because of the situation of the other EVs in the cluster. At minute 719 the EV leaves plug #25 and is replaced by another EV that arrives with a high SoC, is assigned relatively low fuzzy weights during its permanence, so that the battery of the EV connected to plug #25 is charged in the default mode until reaching the maximum SoC and is then no longer available for participating in the coordinated EV charging strategy.

At plug #21, an EV arrives at minute 864, is immediately assigned a high fuzzy weight, and is selected to increase the EV charging power. This EV reaches the maximum SoC at minute 896, then plug #21 is no longer selected (its fuzzy weight decreases to low values and later to zero).

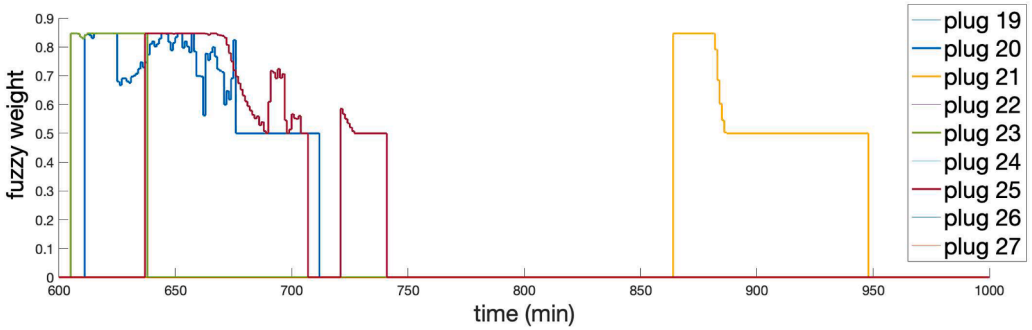

Fig. A1. Fuzzy weights associated to the EV plugs in the EV coordinated charging strategy.

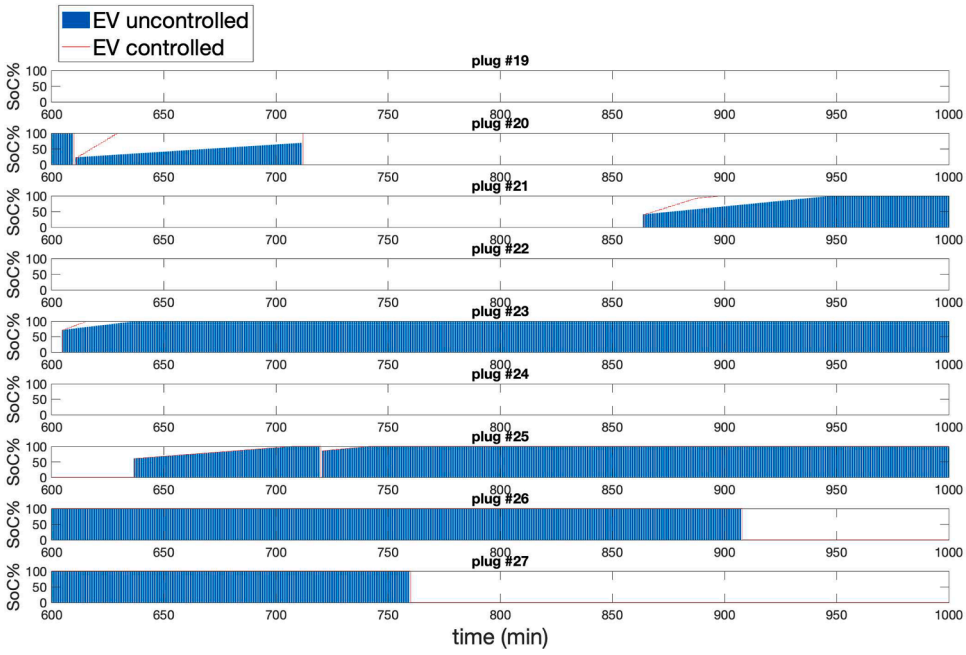

Fig. A2. SoC of the EV batteries connected to the plugs at node #23.

References

[1] S. Ghosh, S. Rahman, M. Pipattanasomporn, Distribution voltage regulation through active power curtailment with PV inverters and solar generation forecasts, IEEE Trans. Sustain. Energy 8 (1) (2017) 13–22.

[2] M.Z. Liu, A.T. Procopiou, K. Petrou, L.F. Ochoa, T. Langstaff, J. Harding, J. Theunissen, On the fairness of PV curtailment schemes in residential distribution networks, IEEE Trans. Smart Grid 11 (5) (2020) 4502–4512. Sept.

[3] E. O'Shaughnessy, J.R. Cruce, K. Xu, Too much of a good thing? Global trends in the curtailment of solar PV, Sol. Energy 208 (2020) 1068–1077.

[4] R. Bayani, S.D. Manshadi, G. Liu, Y. Wang, R. Dai, Autonomous charging of electric vehicle fleets to enhance renewable generation dispatchability, CSEE J. Power Energy Syst. 8 (3) (2022) 669–681.

[5] California ISO, Managing oversupply, [Online] https://www.caiso.com/informed/Pages/ManagingOversupply.aspx (accessed 6 December 2023).

[6] International Energy Agency, Renewable energy market update - outlook for 2023 and 2024, June 2023, [Online] https://www.iea.org/reports/renewable-energy-market-update-june-2023 (accessed 6 December 2023).

[7] F. Olivier, P. Aristidou, D. Ernst, T. Van Cutsem, Active management of low-voltage networks for mitigating overvoltages due to photovoltaic units, IEEE Trans. Smart Grid 7 (2) (2016) 926–936.

[8] M.S.S. Abad, J. Ma, Photovoltaic hosting capacity sensitivity to active distribution network management, IEEE Trans. Power Syst. 36 (1) (2021) 107–117.

[9] R. Udawalpola, T. Masuta, T. Yoshioka, K. Takahashi, H. Ohtake, Reduction of power imbalances using battery energy storage system in a bulk power system with extremely large photovoltaics interactions, Energies 14 (3) (2021) 522, art.

[10] V. Sharma, M.H. Haque, S.M. Aziz, T. Kauschke, Reduction of PV curtailment through optimally sized residential battery storage, in: Proceedings of the IEEE International Conference on Power Electronics, Drives and Energy Systems (PEDES), 2020, pp. 1–6.

[11] T. Masuta, J. Gari da Silva, Fonseca, H. Ootake, A. Murata, Application of battery energy storage system to power system operation for reduction in PV curtailment based on few-hours-ahead PV forecast, in: Proceedings of the IEEE International Conference on Power System Technology (POWERCON), 2016, pp. 1–6.

[12] H. Akutsu, K. Hirata, A. Ohori, N. Hattori, Y. Ohta, Decentralized control approach to power curtailment instruction problem for PV generation plants with storage, in: Proceedings of the 11th Asian Control Conference (ASCC), 2017, pp. 2825–2830.

[13] D. Kim, H. Kim, D. Won, Operation strategy of shared ESS based on power sensitivity analysis to minimize PV curtailment and maximize profit, IEEE Access 8 (2020) 197097–197110.

[14] International Energy Agency (IEA), Global EV Outlook 2022, May 2022, https://www.iea.org/reports/global-ev-outlook-2022.

[15] J.K. Szinai, C.J.R. Sheppard, N. Abhyankar, A.R. Gopal, Reduced grid operating costs and renewable energy curtailment with electric vehicle charge management, Energy Policy 136 (2020) 111051 art.

[16] M. Zeraati, M.E. Hamedani Golshan, J.M. Guerrero, A consensus-based cooperative control of PEV battery and PV active power curtailment for voltage regulation in distribution networks, IEEE Trans. Smart Grid 10 (1) (2019) 670–680.

[17] H. Wang, H. Ma, C. Liu, W. Wang, Optimal scheduling of electric vehicles charging in battery swapping station considering wind- photovoltaic accommodation, Electr. Power Syst. Res. 199 (2021) 107451 art.

[18] R. Das, Y. Wang, G. Putrus, R. Kotter, M. Marzband, B. Herteleer, J. Warmerdam, Multi-objective techno-economic-environmental optimisation of electric vehicle for energy services, Appl. Energy 257 (2020) 113965 art.

[19] L. Wang, A. Dubey, A.H. Gebremedhin, A.K. Srivastava, N. Schulz, MPC-based decentralized voltage control in power distribution systems with EV and PV coordination, IEEE Trans. Smart Grid 13 (4) (2022) 2908–2919.

[20] H. Li, M.A. Azzouz, A.A. Hamad, Cooperative voltage control in MV distribution networks with electric vehicle charging stations and photovoltaic DGs, IEEE Syst. J. 15 (2) (2021) 2989–3000.

[21] A.F. Cortés Borray, J. Merino, E. Torres, A. Garcés, J. Mazón, Centralised coordination of EVs charging and PV active power curtailment over multiple aggregators in low voltage networks, Sustain. Energy Grids Netw. 27 (2021) 100470 art.

[22] H. Kikusato, Y. Fujimoto, S. Hanada, D. Isogawa, S. Yoshizawa, H. Ohashi, Y. Hayashi, Electric vehicle charging management using auction mechanism for reducing PV curtailment in distribution systems, IEEE Trans. Sustain. Energy 11 (3) (2020) 1394–1403.

[23] S. Kanai, S. Tamura, V2G contribution to reduction of renewable energy curtailment by valley-filling approach, in: Proceedings of the IEEE PES Innovative Smart Grid Technologies - Asia (ISGT Asia, 2021, pp. 1–5.

[24] S.M.G. Dumlao, K.N. Ishihara, Impact assessment of electric vehicles as curtailment mitigating mobile storage in high PV penetration grid, Energy Rep. 8 (Supplement 1) (2022) 736–744.

[25] R. Fachrizal, U.H. Ramadhani, J. Munkhammar, J. Widén, Combined PV–EV hosting capacity assessment for a residential LV distribution grid with smart EV charging and PV curtailment, Sustain. Energy Grids Netw. 26 (2021) 100445 art.

[26] M.R. Feizi, M.E. Khodayar, J. Li, Data-driven distributionally robust unbalanced operation of distribution networks with high penetration of photovoltaic generation and electric vehicles, Electr. Power Syst. Res. 210 (2022) 108001 art.

[27] S.W. Park, K.S. Cho, G. Hoefter, S.Y. Son, Electric vehicle charging management using location-based incentives for reducing renewable energy curtailment considering the distribution system, Appl. Energy 305 (2022) 117680 art.

[28] H. Zheng, Y. Ren, Y. Guo, X. Liu, W. Wang, Q. Zhang, D. Zhao, Coordinated charging of electric vehicles in distribution network with high proportion distributed photovoltaic, in: Proceedings of the IEEE 5th Conference on Energy Internet and Energy System Integration (EI2), Taiyuan, China, 2021, pp. 1899–1904.

[29] S. Xia, X. Zhang, L. Yuan, T. Wu, G. Li, M. Shahidehpour, An energy scheduling scheme for highway microgrids virtually networked by electric operation and maintenance vehicles, IEEE Trans. Ind. Appl. 60 (1) (2024) 1010–1022.

[30] Y. Zhou, A.N. Manea, W. Hua, J. Wu, W. Zhou, J. Yu, S. Rahman, Application of distributed ledger technology in distribution networks, Proc. IEEE 110 (12) (2022) 1963–1975.

[31] Y.T. Aklilu, J. Ding, Survey on blockchain for smart grid management, Control, Oper. Energies 15 (2022) 193, art.

[32] J. Ping, Z. Yan, S. Chen, L. Yao, M. Qian, Coordinating EV charging via blockchain, J. Mod. Power Syst. Clean Energy 8 (3) (2020) 573–581.
[33] A. Baggio, F. Grimaccia, Blockchain as key enabling technology for future electric energy exchange: a vision, IEEE Access 8 (2020) 205250–205271.
[34] Y. Xu, Z. Liu, C. Zhang, J. Ren, Y. Zhang, X. Shen, Blockchain-based trustworthy energy dispatching approach for high renewable energy penetrated power systems, IEEE Internet Things J. 9 (12) (2022) 10036–10047.
[35] M.J.A. Baig, M.T. Iqbal, M. Jamil, J. Khan, Blockchain-based peer-to-peer energy trading system using open-source angular framework and hypertext transfer protocol, Electronics 12 (2023) 287, art.
[36] A. Iqbal, A.S. Rajasekaran, G.S. Nikhil, M. Azees, A secure and decentralized blockchain based EV energy trading model using smart contract in V2G network, IEEE Access 9 (2021) 75761–75777.
[37] M. Mylrea, S.N.G. Gourisetti, Blockchain for smart grid resilience: exchanging distributed energy at speed, scale and security, in: Proceedings of the Resilience Week (RWS), Wilmington, DE, USA, 2017, pp. 18–23.
[38] C. Liu, K.K. Chai, X. Zhang, E.T. Lau, Y. Chen, Adaptive blockchain-based electric vehicle participation scheme in smart grid platform, IEEE Access 6 (2018) 25657–25665.
[39] H. Liu, Y. Zhang, S. Zheng, Y. Li, Electric vehicle power trading mechanism based on blockchain and smart contract in V2G network, IEEE Access 7 (2019) 160546–160558.
[40] X. Chen, T. Zhang, W. Ye, Z. Wang, H.H.C. Iu, Blockchain-based electric vehicle incentive system for renewable energy consumption, in: Proceedings of the IEEE Transactions on Circuits and Systems II: Express Briefs 68, 2021, pp. 396–400.
[41] N. Chanthong, T. Ruangsakorn, S. Glomglome, Blockchain and smart contract payment for electric vehicle charging, in: Proceedings of the 17th International Conference on Electrical Engineering/Electronics, Computer, Telecommunications, and Information Technology (ECTI-CON), 2020, pp. 161–164.
[42] S. Guo, K. Wang, Y. Li, Z. Yan, X. Xia, An electric vehicle charging transaction model based on blockchain, in: Proceedings of the International Conference on Blockchain Technology and Information Security (ICBCTIS), 2022, pp. 147–150.
[43] S. Jeong, N.N. Dao, Y. Lee, C. Lee, S. Cho, Blockchain based billing system for electric vehicle and charging station, in: Proceedings of the Tenth International Conference on Ubiquitous and Future Networks (ICUFN), 2018, pp. 308–310.
[44] Y.J. Lin, Y.C. Chen, J.Y. Zheng, D.W. Shao, D. Chu, H.T. Yang, Blockchain-based intelligent charging station management system platform, IEEE Access 10 (2022) 101936–101956.
[45] G.C. Okwuibe, Z. Li, T. Brenner, O. Langniss, A blockchain based electric vehicle smart charging system with flexibility, IFAC-PapersOnLine 53 (2) (2020) 13557–13561.
[46] S. Saadatmandi, G. Chicco, A. Favenza, H. Mirtaheri, M. Arnone, Exploiting blockchain for smart charging of electric vehicles: a proof of Stake algorithm, in: Proceedings of the 1st Workshop on BLOckchain for Renewables INtegration (BLORIN 2022), Palermo, Italy, 2022, 2–3 Sept.
[47] Y. Zhang, J. Xu, L. Zhu, A comprehensive survey on consensus mechanism of blockchain, J. Netw. Comput. Appl. 126 (2019) 50–70.
[48] K. Mahmoud, M. Abdel-Nasser, M. Lehtonen, Low-computational voltage-assessment approach considering fine-resolution simulations for distribution systems with photovoltaics, IEEE Syst. J. 15 (4) (2021) 5321–5331.
[49] S. Saadatmandi, G. Chicco, F. Giordano, M. Arnone, Reducing the curtailment of photovoltaic energy production through smart electric vehicle charging, in: Proceedings of the AEIT International Annual Conference (AEIT), Rome, Italy, 2022, pp. 1–6.
[50] Y. Salgado Duarte, J. Szpytko, A.M. del Castillo Serpa, Monte Carlo simulation model to coordinate the preventive maintenance scheduling of generating units in isolated distributed power systems, Electr. Power Syst. Res. 182 (2020) 106237 art.
[51] I.M. Sobol, A Primer for the Monte Carlo Method, CRC Press, Boca Raton, FL, USA, 1994.
[52] R. Burch, F.N. Najm, P. Yang, T.N. Trick, A Monte Carlo approach for power estimation, IEEE Trans. Very Large Scale Integr. VLSI Syst. 1 (1) (1993) 63–71.
[53] M. Bicher, M. Wastian, D. Brunmeir, N. Popper, Review on Monte Carlo simulation stopping rules: how many samples are really enough? Simul. Notes Eur. 32 (1) (2022) 1–8.
[54] F.J. Hickernell, S.C.T. Choi, L. Jiang, L. Antoni, J. Rugama, Monte Carlo simulation, automatic stopping criteria for. Wiley StatsRef: Statistics Reference Online, John Wiley & Sons, Ltd, 2018, https://doi.org/10.1002/9781118445112.stat08035.
[55] M.R. Anderberg, Cluster Analysis for Applications, Academic Press, New York, 1973.
[56] E.H. Mamdani, S. Assilian, An experiment in linguistic synthesis with a fuzzy logic controller, Int. J. Man Mach. Stud. 7 (1) (1975) 1–13.
[57] A. Sadollah, Introductory chapter: which membership function is appropriate in fuzzy system?. Fuzzy Logic Based in Optimization Methods and Control Systems and Its Applications InTech, 2018 https://doi.org/10.5772/intechopen.79552. Oct. 31.
[58] L.A. Zadeh, Fuzzy sets, Inf. Control. 8 (1965) 338–353.
[59] C. Pop, T. Cioara, M. Antal, I. Anghel, I. Salomie, M. Bertoncini, Blockchain based decentralized management of demand response programs in smart energy grids, Sensors 18 (2018) 162, art.
[60] A. Afif Monrat, O. Schelén, K. Andersson, Blockchain mobility solution for charging transactions of electrical vehicles, in: Proceedings of the IEEE/ACM 13th International Conference on Utility and Cloud Computing (UCC), Leicester, UK, 2020.
[61] M.A. Manolache, S. Manolache, N. Tapus, Decision making using the blockchain proof of authority consensus, Procedia Comput. Sci. 199 (2022) 580–588.
[62] K.P. Schneider, B.A. Mather, B.C. Pal, C.W. Ten, G.J. Shirek, H. Zhu, J.C. Fuller, J.L. R. Pereira, L.F. Ochoa, L.R. de Araujo, R.C. Dugan, S. Matthias, S. Paudyal, T. E. McDermott, W. Kersting, Analytic considerations and design basis for the IEEE distribution test feeders, IEEE Trans. Power Syst. 33 (3) (2018) 3181–3188.
[63] The IEEE, IEEE PES Test Feeder, [online] https://cmte.ieee.org/pes-testfeeders/resources/(accessed 6 December 2023).
[64] H. Ren, R.R. Jha, A. Dubey, N. Schulz, Extremum-seeking adaptive droop for model-free and localized volt-var optimization, IEEE Trans. Power Syst. 37 (1) (2022) 179–190.
[65] A. Mazza, G. Chicco, High-quality load pattern reconstruction from smart meter data to enhance the assessment of peak power and network losses, IEEE Trans. Ind. Appl. 58 (3) (2022) 3261–3274.